

## $\beta$ -Arrestin 1 and 2 similarly influence $\mu$ -opioid receptor mobility and distinctly modulate adenylyl cyclase activity

Vendula Markova<sup>a</sup>, Lucie Hejnova<sup>a</sup>, Ales Benda<sup>b</sup>, Jiri Novotny<sup>a,\*</sup>, Barbora Melkes<sup>a</sup>

<sup>a</sup> Department of Physiology, Faculty of Science, Charles University, Prague, Czech Republic

<sup>b</sup> IMCF at Biocev, Faculty of Science, Charles University, Prague, Czech Republic

### ARTICLE INFO

#### Keywords:

Adenylyl cyclase  
 $\beta$ -Arrestin  
 $\mu$ -Opioid receptor  
 Receptor lateral mobility  
 DAMGO  
 Endomorphin-2

### ABSTRACT

$\beta$ -Arrestins are known to play a crucial role in GPCR-mediated transmembrane signaling processes. However, there are still many unanswered questions, especially those concerning the presumed similarities and differences of  $\beta$ -arrestin isoforms. Here, we examined the roles of  $\beta$ -arrestin 1 and  $\beta$ -arrestin 2 at different levels of  $\mu$ -opioid receptor (MOR)-regulated signaling, including MOR mobility, internalization of MORs, and adenylyl cyclase (AC) activity. For this purpose, naïve HEK293 cells or HEK293 cells stably expressing YFP-tagged MOR were transfected with appropriate siRNAs to block in a specific way the expression of  $\beta$ -arrestin 1 or  $\beta$ -arrestin 2. We did not find any significant differences in the ability of  $\beta$ -arrestin isoforms to influence the lateral mobility of MORs in the plasma membrane. Using FRAP and line-scan FCS, we observed that knockdown of both  $\beta$ -arrestins similarly increased MOR lateral mobility and diminished the ability of DAMGO and endomorphin-2, respectively, to enhance and slow down receptor diffusion kinetics. However,  $\beta$ -arrestin 1 and  $\beta$ -arrestin 2 diversely affected the process of agonist-induced MOR endocytosis and exhibited distinct modulatory effects on AC function. Knockdown of  $\beta$ -arrestin 1, in contrast to  $\beta$ -arrestin 2, more effectively suppressed forskolin-stimulated AC activity and prevented the ability of activated-MORs to inhibit the enzyme activity. Moreover, we have demonstrated for the first time that  $\beta$ -arrestin 1, and partially  $\beta$ -arrestin 2, may somehow interact with AC and that this interaction is strongly supported by the enzyme activation. These data provide new insights into the functioning of  $\beta$ -arrestin isoforms and their distinct roles in GPCR-mediated signaling.

### 1. Introduction

Signaling pathways initiated by different cell surface receptors form complex networks that play an essential role in many cellular events like proteostasis, cell differentiation, apoptosis, *etc.* In this respect, G protein-coupled receptors (GPCRs) represent one of the most studied membrane-bound receptor families [1]. Investigation of these receptors and their signaling systems turned out to be very useful for identifying new potential targets for therapeutic opportunities. One of the well-known signaling actions regulated by many GPCRs is activation/inhibition of adenylyl cyclase (AC) that catalyzes formation of cyclic AMP, a key second messenger in numerous signal transduction pathways [2]. Another important effect of activation of GPCRs is  $\beta$ -arrestin recruitment, signaling, and subsequent receptor internalization [3].

$\beta$ -Arrestins are important signaling and scaffold proteins that are nowadays extensively studied. These molecules are also known to act as multifunctional adaptor proteins binding many non-receptor proteins to

control multiple signaling pathways. An increasing number of studies have also demonstrated the scaffolding roles of  $\beta$ -arrestins in both physiological and pathological conditions [4]. In GPCR signaling,  $\beta$ -arrestins play a key role in turning-off the coupling of the receptors to heterotrimeric G proteins and thereby inhibit the receptor-mediated signaling process. They also regulate GPCR trafficking as well as G protein-independent signaling *via* MAPK pathways [5]. There are two ubiquitously expressed  $\beta$ -arrestin isoforms,  $\beta$ -arrestin 1 and  $\beta$ -arrestin 2, which share many common features [6]. The overall structures of  $\beta$ -arrestin 1 and  $\beta$ -arrestin 2 are similar. Both these proteins have nuclear localization sequences at the N terminus, but  $\beta$ -arrestin 2 additionally has a C-terminal nuclear export signal. Consequently,  $\beta$ -arrestin 1 in its inactive state can be found both in the nucleus and cytoplasm and  $\beta$ -arrestin 2 only in the cytoplasm. After activation, they both are transported either to the nucleus or plasma membrane [7]. The signaling functionality of  $\beta$ -arrestin 1 and 2 was lately interpreted by analyzing the physical interactomes of these multidimensional transducers. When

\* Corresponding author.

E-mail address: [jiri.novotny@natur.cuni.cz](mailto:jiri.novotny@natur.cuni.cz) (J. Novotny).

looking at the distribution of interaction partners of  $\beta$ -arrestin isoforms, a stronger representation of plasma membrane-associated binding partners for  $\beta$ -arrestin 1 can be found when compared to  $\beta$ -arrestin 2 [8].  $\beta$ -Arrestin 1 binding partners are more connected with G protein-associated processes and cell cycle regulation, compared to  $\beta$ -arrestin 2. However, with a rich closely associated functional network of activities,  $\beta$ -arrestin 2 may control a more coherent signaling response away from plasma membrane-bound receptors [8]. Hence,  $\beta$ -arrestin isoforms can apparently function in distinct ways. At this time, our understanding of the differences between these two related proteins and their signaling mechanisms is far from complete and there is still much work to be done in this field.

Here, we set out to investigate the presumed similarities and differences between  $\beta$ -arrestin 1 and  $\beta$ -arrestin 2 with respect to their interaction with  $\mu$ -opioid receptors (MORs) and the possible impact on adenylyl cyclase (AC) signaling. A couple of research studies determined that  $\beta$ -arrestins may play an important role in MOR-mediated signaling. In most of these studies, attention has been devoted primarily to  $\beta$ -arrestin 2 as a key modulator of MOR-mediated events [9–11]. The possible role of  $\beta$ -arrestin 1 in MOR signaling has not yet been fully explored. It is important to highlight that MOR agonists exhibit biased agonism and the outcome of MOR-mediated signaling events depends, to a large extent, on the ligand used [12]. Thus, we suspect that AC activity might also be diversely affected by biased MOR agonists. However, there are currently no data to support this notion.

MORs are typically coupled to the inhibitory G proteins [13]. There are two principal ways in which heterotrimeric G proteins can regulate AC function. This enzyme is either directly activated or inhibited by the  $G_{\alpha s}$  and  $G_{\alpha i}$  subunits, respectively, or by the  $G_{\beta\gamma}$  dimer, which can be either stimulatory or inhibitory depending on the AC isoform [14]. Nevertheless, activity of AC can be affected in a number of different ways, apart from G proteins. Traditionally, a labdane diterpene forskolin has been used as a compound that directly activates AC [15]. Forskolin-stimulated AC activity can serve as a useful means for facilitating the assessment of functional coupling of Gi-linked receptors to AC. It should be noted that the potential involvement of  $\beta$ -arrestin isoforms in modulating AC activity has not yet been clearly elucidated. There are some indications that  $\beta$ -arrestins may exhibit blocking effects on AC activity regulated by G proteins through the inhibition of receptor–G protein coupling [16,17]. However, it is not known whether  $\beta$ -arrestins might have a direct effect on AC. Therefore, in this work, we wanted to find out if and how  $\beta$ -arrestins interact with this enzyme and affect AC signaling.

## 2. Materials and methods

### 2.1. Materials

Fetal bovine serum (FBS) was purchased from Thermo Fisher Scientific (Waltham, MA, USA) and Lipofectamine RNAiMAX and Lipofectamine 3000 reagents were from Invitrogen (Carlsbad, CA, USA). The HTRF cAMP kits were purchased from Cisbio Bioassays (Codolet, France), [ $^3$ H]DAMGO from American Radiolabeled Chemicals (Saint Louis, MO, USA) and Dynabeads Co-Immunoprecipitation kit was from Life Technologies (Carlsbad, CA, USA). Nitrocellulose membrane was obtained from GE Healthcare (Chicago, IL, USA) and SuperSignal West Dura chemiluminescent detection reagent was from Pierce Biotechnology (Rockford, IL, USA). All other chemicals were purchased from Sigma-Aldrich (St. Louis, MI, USA) and were of the highest purity grade.

### 2.2. Cell culture and ligands

HEK293 and HMY-1 cells (HEK293 cells stably expressing MOR-YFP) were routinely cultured in DMEM supplemented with 10% FBS, 1% AAS (antibiotic antimycotic solution), and, in the case of HMY-1 cells, in the presence of 800  $\mu$ g/ml G418 sulfate. Cells were kept at 37 °C in a

humidified atmosphere containing 5% CO<sub>2</sub>. The generation of the HMY-1 cell line was previously described [18]. The YFP tag was localized at the C-terminus of MOR.

MOR ligands used in this study comprised DAMGO, endomorphin-2, and morphine and all these compounds were used at a concentration of 1  $\mu$ M, if not stated otherwise. The  $\beta$ -AR agonist isoprenaline was used at a concentration of 1  $\mu$ M.

### 2.3. siRNA transfection

Cells were seeded in culture medium at an appropriate density into plastic multiwell plates of the desired well format. Twenty-four hours after seeding, cells were transfected with appropriate siRNA oligos or scrambled siRNA (as a negative control) using Lipofectamine® RNAiMAX reagent according to manufacturers' instructions. siRNAs for silencing of  $\beta$ -arrestin 1 (sc-29741),  $\beta$ -arrestin 2 sc-29208, and  $G_{\alpha s}$  (sc-29328) were purchased from Santa Cruz Biotechnology) and Silencer™ SelectNegative Control No. 2 siRNA (#4390847) was from ThermoFisher Scientific. Briefly, both siRNA and Lipofectamine were diluted in optiMEM medium and incubated for 5 min at room temperature. Then, the mixture was added to the cells and incubated for 24 h (if not stated otherwise) before proceeding with any further experiments.

### 2.4. Fluorescence recovery after photobleaching

Fluorescence recovery after photobleaching (FRAP) on live cells was carried out as described previously [18]. Briefly, HMY-1 cells were seeded on glass-bottom dishes in phenol red-free media supplemented with 10% FBS, 1% AAS, and 800  $\mu$ g/ml G418. FRAP was performed on cells placed in a live-cell imaging chamber using a confocal laser scanning microscope Zeiss LSM 880 (Carl Zeiss AG, Oberkochen, Germany) equipped with the ibidi heating and gas incubation system (37 °C, 5% CO<sub>2</sub>, and 90% humidity). The data were collected from at least 50 cells in 3 independent experiments. Yellow fluorescent protein (YFP) was excited using a 514 nm Argon laser. Ligands were added to the cell culture and data were acquired after 10 min of incubation. The data were analyzed using easyFRAP, a MATLAB platform-based tool [19].

### 2.5. Line-scan fluorescence correlation spectroscopy

Line-scan fluorescence correlation spectroscopy (FCS) data were acquired on Zeiss LSM 880 inverted point scanning confocal microscope, using 63 $\times$  NA1.4 oil immersion objective, 5 uW of 488 nm laser at the sample plane, 500–550 nm window of 32-channel GaAsP spectral detector operated at single-photon counting mode, and pinhole size 1 AU. First, the cell was localized using standard CLSM imaging. A suitable area of plasma membrane close to the coverslip, free of visible structures, was selected, properly focused, and zoomed to the size 6  $\times$  6  $\mu$ m<sup>2</sup>. A 6  $\mu$ m long line was selected for fast xt scan (256 pixels with 20 nm pixel size, bidirectional scan with maximum possible (15 in ZEN software) scanning frequency 2 kHz, 200,000 lines corresponding to 30 s). The data were collected from at least 45 cells in 3 independent experiments. Acquired data were exported as \*.ism5 files and analyzed in home-written "LS-FCS data analysis" software (user interface developed in LabVIEW2016 (NI), a custom written dll library for fast calculation of spatio-temporal correlations was developed in C/C++ (MVS2015, Microsoft)). The xt scan image data were converted into the single-photon stream and further processed as outlined in Benda et al., 2015 [20]. The resulting spatio-temporal correlations were fitted by non-weighted NLSF using a model assuming one component free lateral (2D) diffusion, Gaussian point spread function and fast photophysical dynamics (Eq. (1)).

$$g(t, \delta) = g_{\infty} + \frac{1}{N \cdot [1 - F_{pp}]} \left[ 1 - F_{pp} \cdot \left( 1 - e^{-\frac{t}{t_{pp}}} \right) \right] \frac{1}{4Dt + \omega^2} e^{-\frac{\delta^2}{4Dt + \omega^2}} \quad (1)$$

where  $t$  denotes correlation time,  $\delta$  is the distance,  $g_{\infty}$  is the constant offset, usually equal to 1,  $N$  is the average number of diffusing entities within the Gaussian detection area,  $D$  is the diffusion coefficient,  $\omega$  is the radius of the Gaussian profile,  $F_{pp}$  is the fraction of molecules in dark state and  $t_{pp}$  is the time constant for switching between bright and dark states. The read-out parameters include absolute lateral diffusion coefficient, size of the detection area, the concentration of labeled diffusing particles, and when combined with intensity trace, the brightness of the diffusing particles.

## 2.6. Assessment of MOR internalization

HMY-1 cells were seeded in a 24-well plate (250,000 cells/well) and after 24 h cells were transfected with relevant siRNA. The next day, cells were treated for different time intervals (0, 5, 10, 20, and 30 min) with appropriate ligands at a concentration of 1  $\mu$ M. After incubation at 37 °C, the culture plate was put on ice and cells were washed once with 500  $\mu$ l of ice-cold PBS. Washed cells were incubated for 1 min with ice-cold acid/salt solution (0.5 M NaCl, 0.2 M acetic acid; pH 2.5) in order to release the ligand from cell surface MORs. After incubation, cells were washed twice with ice-cold PBS and further incubated with 10 nM [<sup>3</sup>H] DAMGO dissolved in serum-free DMEM and 1% BSA for 120 min at 0 °C (on ice). After incubation, the cells were harvested using a Brandel cell harvester (Gaithersburg, MD, USA). The radioactivity was determined by liquid scintillation counting. Nonspecific binding was assessed in parallel wells containing 100  $\mu$ M naloxone.

## 2.7. Determination of cAMP

The measurement of cAMP production modulated by forskolin, isoprenaline, DAMGO, morphine and edomorphin-2 was performed using cAMP-Gs Dynamic kit and cAMP-Gi kit based on homogeneous time-resolved fluorescence (HTRF) technology (Cisbio). In the case of pertussis toxin (PTX), HMY-1 cells were treated with 25 ng/ml of PTX for 24 h before the experiment. Briefly, appropriately transfected cells were firstly dispensed into 384-well microplates and incubated in stimulation buffer supplemented with 0.5  $\mu$ M 3-isobutyl-1-methylxanthine (a non-specific inhibitor of cAMP and cGMP phosphodiesterases) in the presence of appropriate ligands at a concentration of 1  $\mu$ M for 20 min (if not stated otherwise) at 37 °C. After this incubation period, in the case of cAMP-Gi kit, forskolin was added to the wells to obtain a final concentration of 2  $\mu$ M, and cells were incubated for 45 min at 37 °C. Thereafter, d2-labeled cAMP and monoclonal anti-cAMP Europium cryptate-labeled antibody were diluted in lysis buffer and added to the reaction mixture as described by the manufacturer. After 1 h of incubation at room temperature (RT), the lysed cells were transferred into a 96-well white plate, and the fluorescence at 620 nm and 665 nm was measured on a plate reader (CLARIOStar, BMG Labtech). The time-resolved FRET counts were expressed as the ratio of the acceptor (665 nm) and donor (620 nm) emission signals. The ratio was converted to the concentration of cAMP using a calibration curve. As a rule, basal cAMP concentration was considered as 0% cAMP generation. In the case of cAMP-Gi kit, maximal cAMP generation by forskolin in control cells was considered as 100%. The highest cAMP level generated by forskolin or isoprenaline in control cells was considered as 100% in the case of cAMP-Gs Dynamic kit.

## 2.8. Co-immunoprecipitation and western blot analyses

HEK293 cells were seeded in tissue culture plates and subsequently transfected with  $\beta$ -arrestin 1-HA tag (pcDNA3 barr1 HA was a gift from

Robert Lefkowitz (Addgene plasmid #14693; <http://n2t.net/addgene:14693>; RRID: Addgene\_14693)) or  $\beta$ -arrestin 2-HA tag (pcDNA3 barr2

HA was a gift from Robert Lefkowitz (Addgene plasmid #14692; <http://n2t.net/addgene:14692>; RRID: Addgene\_14692)) [21] using Lipofectamine® 3000 reagent according to the manufacturer's instructions. Briefly, the diluted plasmid DNA was combined with the diluted Lipofectamine in optiMEM medium (a total volume of 100  $\mu$ l), mixed gently, and then incubated for 15 min. Afterwards, the mixture was added to the cells and incubated for 24 h before proceeding to the next step.

Co-immunoprecipitation (Co-IP) was performed using Dynabeads Co-IP kit according to the manufacturer's instructions. Cells were harvested and cell pellets mixed in a ratio of 1:9 (w/v) with a lysis buffer (1xIP, 200 mM NaCl, 0.5% Triton X-100, and Complete EDTA-free protease inhibitor cocktail). The lysis proceeded on ice for 15 min and the samples were subsequently centrifuged at 2600  $\times$ g for 5 min at 4 °C to remove large cell debris and nuclei. The supernatant was used immediately for Co-IP. AC antibody (sc-377243; Santa Cruz Biotechnology) were covalently coupled (7  $\mu$ g/mg) to Dynabeads® M-270 Epoxy beads. The antibody diluted in C1 buffer was mixed with the beads in an Eppendorf tube and after addition of C2 buffer incubated overnight at 37 °C on a rotary shaker. The beads were collected using DynaMag™-2 magnet and washed according to the user instructions. For Co-IP, 1.5 mg of antibody-coupled beads per sample were mixed with cell lysate and rotated at 4 °C for 30 min. The beads were washed in extraction buffer and last wash buffer (LWB) using DynaMag™-2 magnet and then resuspended in elution buffer (EB). The beads were rotated for 5 min at RT. The supernatant containing eluted purified proteins was used for western blot analysis. The resulting immunoblot signal was normalized to the weight of the lysates.

For sodium dodecyl sulfate-polyacrylamide gel electrophoresis (SDS-PAGE), samples of homogenized cells (or proteins eluted from magnetic beads after Co-IP) were solubilized in a Laemmli sample buffer and loaded onto 10% polyacrylamide gels. Following electrophoretic separation, proteins were transferred to a nitrocellulose membrane. The nitrocellulose membrane was blocked with nonfat dry milk in TBS buffer (10 mM Tris, 150 mM NaCl; pH 8) for 30 min and then incubated with primary antibody against AC (sc-377,243; Santa Cruz Biotechnology), HA-probe (sc-7392; Santa Cruz Biotechnology),  $\beta$ -arrestin 1 (D8O3J; Cell Signaling) or  $\beta$ -arrestin 2 (PA1-732; Invitrogen) and rocked overnight at 4 °C. After three 10-min washes in TBS-T buffer (TBS containing 0.3% Tween-20), the membrane was incubated with appropriate secondary HRP-conjugated antibody for 1 h at RT. The membrane was washed three times for 10 min in TBS-T buffer and protein bands visualized using enhanced chemiluminescence (ECL) according to the manufacturer's instructions. Western blots were scanned with high resolution CCD scanner (EPSON Perfection V600 Photo) and quantitatively analyzed using ImageJ software.

## 2.9. Statistics

Results were analyzed using GraphPad Prism (version 6.0). Data are presented as mean values  $\pm$  standard error of the mean (S.E.M.) of at least three independent experiments. One-way ANOVA, followed by a *post hoc* Bonferroni test, was used to examine whether there was a significant difference between groups. Statistical significance was defined as  $p < 0.05$ .

## 3. Results

### 3.1. $\beta$ -Arrestins influence the lateral mobility of MORs in the plasma membrane

The lateral mobility of GPCRs in the plasma membrane can be affected by many different factors. Among the most widely studied factors are receptor interactions with other proteins and lipids, as well as

receptor activation by different ligands [18,22–24]. Here, we conducted a set of experiments in which we determined the lateral mobility of MOR-YFP using two different types of microscopy techniques: FRAP (Fig. 1) and line-scan FCS (Fig. 2). Both these techniques are suitable for measuring the diffusion coefficient ( $D$ ) of fluorescently tagged molecules and their application ranges largely overlap [25].

FRAP was performed on the plasma membrane-associated pool of MOR-YFP in HMY-1 cells after activation of MORs with opioid agonists (DAMGO, endomorphin-2 and morphine) at a concentration of 1  $\mu$ M. In some experiments, HMY-1 cells were transfected with  $\beta$ -arrestin-specific siRNAs in order to selectively suppress the expression of  $\beta$ -arrestin isoforms. Silencing efficiency was confirmed by Western blotting; the expression level of  $\beta$ -arrestin 1 and  $\beta$ -arrestin 2 fell to  $35\% \pm 4.9\%$  and  $10\% \pm 5\%$ , respectively, as compared to control cells (Suppl. Fig. S1). Representative FRAP curves showing the recovery of fluorescence with time after the photobleach are shown in Fig. 1A–C. Knockdown of either of  $\beta$ -arrestin isoforms led to a significant increase in the lateral mobility of MOR-YFP in resting (control) conditions (Fig. 1D). The movement of the receptor increased by about 25% in HMY-1 cells expressing lower levels of  $\beta$ -arrestin 1 (HMY-1/ $\beta$ -Arr1<sup>(↓)</sup>;  $D = 0.49 \pm 0.02 \mu\text{m}^2/\text{s}$ ) or

$\beta$ -arrestin 2 (HMY-1/ $\beta$ -Arr2<sup>(↓)</sup>;  $D = 0.50 \pm 0.02 \mu\text{m}^2/\text{s}$ ), compared to control cells ( $D = 0.39 \pm 0.02 \mu\text{m}^2/\text{s}$ ). Intriguingly, knockdown of either of  $\beta$ -arrestin isoforms suppressed the ability of DAMGO and endomorphin-2 to increase or decrease, respectively, the rate of lateral movement of MOR-YFP (Fig. 1D). Interestingly, morphine did not have any significant effect on the  $D$  value, either in HMY-1 cell or in cells with depleted  $\beta$ -arrestins (Fig. 1D). Whereas MOR-YFP lateral mobility was increased by about 36% by DAMGO ( $D = 0.53 \pm 0.03 \mu\text{m}^2/\text{s}$ ) and decreased about 39% by endomorphin-2 ( $D = 0.24 \pm 0.03 \mu\text{m}^2/\text{s}$ ) in HMY-1 cells, these opioid agonists did not significantly affect the  $D$  value of MOR-YFP in HMY-1/ $\beta$ -Arr1<sup>(↓)</sup> and HMY-1/ $\beta$ -Arr2<sup>(↓)</sup> cells (Fig. 1D). Interestingly, DAMGO and endomorphin-2 did not change the proportion of mobile and immobile MOR-YFP in HMY-1 cells but both these ligands significantly reduced the receptor mobile fraction after knockdown of both  $\beta$ -arrestin isoforms (Fig. 1E).

Next, we were interested in learning whether the changes in MOR-YFP movement observed after receptor activation or knockdown of  $\beta$ -arrestins can also be detected using the line-scan FCS method. HMY-1 cells were treated in the same way as for FRAP measurements. Typical spatiotemporal correlation curves reflecting the rate of diffusion of

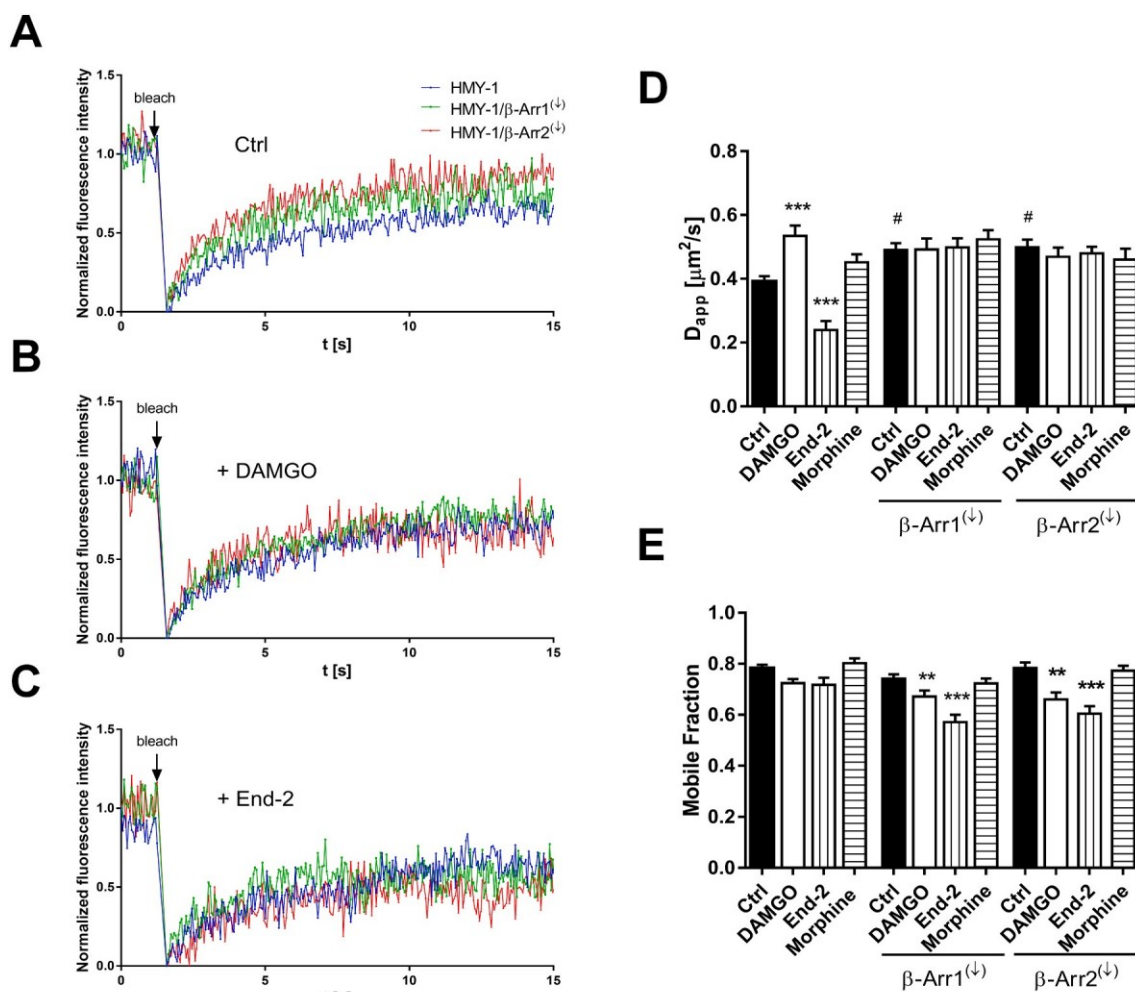


**Fig. 1.** FRAP measurements of the effect of knockdown of  $\beta$ -arrestin 1 and  $\beta$ -arrestin 2 on the lateral mobility of MOR-YFP in the plasma membrane of HMY-1 cells. Cells grown on glass-bottom wells were transfected with specific siRNA for  $\beta$ -arrestin 1 ( $\beta$ -Arr1) or  $\beta$ -arrestin 2 ( $\beta$ -Arr2) and, the following day, FRAP experiments were carried out on control cells (Ctrl) and cells pretreated with DAMGO (1  $\mu$ M), endomorphin-2 (End-2, 1  $\mu$ M) or morphine (1  $\mu$ M) for 10 min. Cell images were acquired of the lower plasma membrane adjacent to the glass support using a Zeiss LSM 880 confocal microscope. Representative examples of normalized fluorescence recovery curves showing the intensity over time in the bleach ROI in control HMY-1 cells and cells lacking  $\beta$ -Arr1 (HMY-1/ $\beta$ -Arr1<sup>(↓)</sup>) or  $\beta$ -Arr2 (HMY-1/ $\beta$ -Arr2<sup>(↓)</sup>) under resting conditions (A) and in the presence of DAMGO (B) or End-2 (C). Panels D and E summarize the pooled data for the apparent diffusion coefficient  $D_{app}$  and percentage mobile fraction, respectively. Data was collected from at least 60 cells and 3 independent experiments. Results are expressed as mean  $\pm$  SEM (\*\* $p < 0.01$ , \*\*\* $p < 0.001$  versus respective Ctrl; # $p < 0.05$  versus untreated Ctrl).

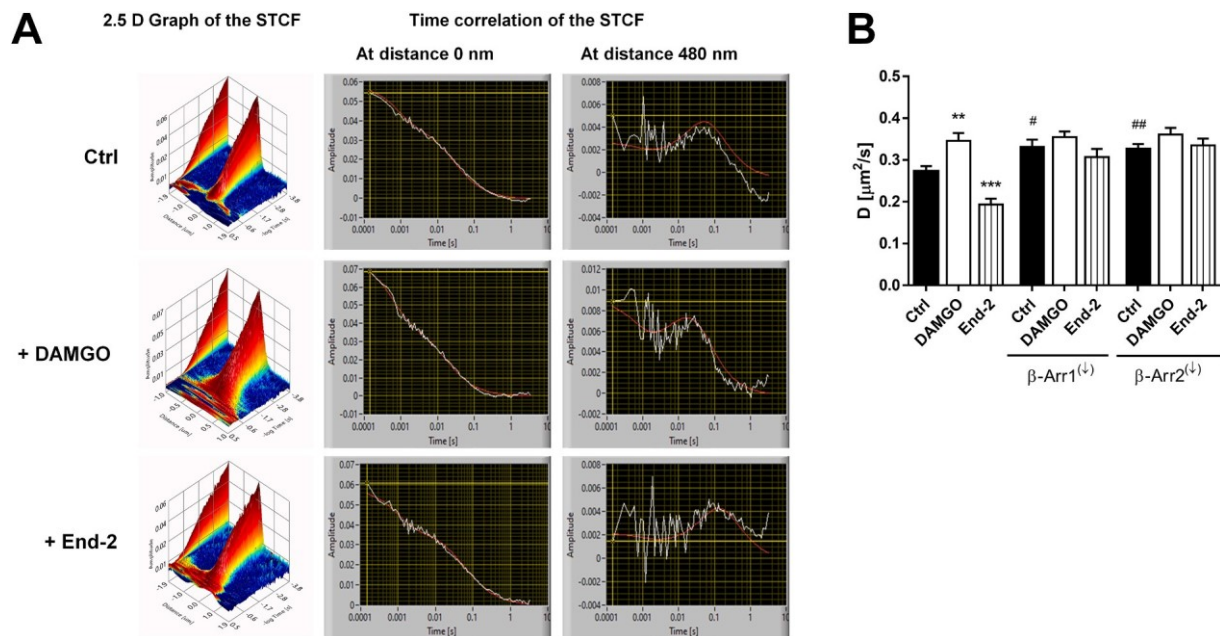


**Fig. 2.** Line-scan FCS measurements of the effect of knockdown of  $\beta$ -arrestin 1 and  $\beta$ -arrestin 2 on the lateral mobility of MOR-YFP in the plasma membrane of HMY-1 cells. Cells grown on glass-bottom wells were transfected with specific siRNA for  $\beta$ -arrestin 1 ( $\beta$ -Arr1) or  $\beta$ -arrestin 2 ( $\beta$ -Arr2) and, the following day, FCS experiments were carried out on control cells (Ctrl) and cells pretreated with DAMGO (1  $\mu$ M) or endomorphin-2 (End-2, 1  $\mu$ M) for 10 min. Cell images were acquired of the lower plasma membrane adjacent to the glass support using a Zeiss LSM 880 confocal microscope. The total length of the scanned line was 6  $\mu$ m. (A) Representative graphs showing the spatio-temporal time correlation function (STCF) in HMY-1 cells untreated and treated with DAMGO or End-2. Panel D summarizes the pooled data for the diffusion coefficient  $D$  under different experimental conditions. Data was collected from at least 60 cells and 3 independent experiments. Results are expressed as mean  $\pm$  SEM (\*\* $p$  < 0.01, \*\*\* $p$  < 0.001 versus respective Ctrl; # $p$  < 0.05, ## $p$  < 0.01 versus untreated Ctrl).

MOR-YFP at a distance of 480 nm are shown in Fig. 2A. DAMGO and endomorphin-2 changed MOR-YFP mobility in the plasma membrane of HMY-1 cells in opposite directions, which was absolutely in line with the results obtained by FRAP. Knockdown of  $\beta$ -arrestin 1 or  $\beta$ -arrestin 2 increased the  $D$  value of MOR-YFP by about 22% and this manipulation eliminated the ability of both opioid agonists to affect receptor lateral movement (Fig. 2B). This is fully consistent with the observations made using FRAP. Although there were certain differences in the  $D$  values obtained by FRAP and line-scan FCS, both these methods provided highly comparable results.

### 3.2. $\beta$ -Arrestin 1 and 2 uniquely affect agonist-induced MOR internalization

Activation of MOR-YFP by DAMGO or endomorphin-2 resulted in receptor translocation from the plasma membrane into the cell interior. The redistribution of the fluorescence signal of MOR-YFP was clearly detectable by confocal microscopy within 5 min after the addition of either of opioid ligands to HMY-1 cells (Fig. 3A). To quantify the number of MORs remaining at the plasma membrane after treatment with DAMGO or endomorphin-2, radioligand binding assays were performed on intact cells. HMY-1 cells were seeded into a 24-well plate and transfected with  $\beta$ -arrestin 1 or  $\beta$ -arrestin 2 siRNA. The cells were then incubated with DAMGO or endomorphin-2 for different time intervals (5–30 min). These two opioid ligands differed markedly in their capacity to internalize MORs. The number of plasma membrane-bound MOR per cell at each time point was calculated from original [<sup>3</sup>H]DAMGO binding data. After 30 min treatment with DAMGO, more than 50% of MORs disappeared from the plasma membrane of HMY-1 cells (Fig. 3C). On the other hand, incubation of HMY-1 cells with endomorphin-2 for the same time period resulted in the disappearance of about 24% of MORs (Fig. 3D). Knockdown of  $\beta$ -arrestin 1 or 2 prevented maximal internalization of MORs by DAMGO; about 77% of MORs remained associated with the plasma membrane even after 30 min under these conditions

(Fig. 3C). The time course of redistribution of MOR in HMY-1/ $\beta$ -Arr2<sup>(↓)</sup> cells with diminished  $\beta$ -arrestin 2 expression which were treated with endomorphin-2 was not significantly changed compared to HMY-1 cells. Interestingly, downregulation of  $\beta$ -arrestin 1 in HMY-1/ $\beta$ -Arr1<sup>(↓)</sup> cells diminished the internalization of MORs after 20 min of treatment with End-2 compared to control cells or cells with downregulated  $\beta$ -arrestin 2.

### 3.3. Attenuation of adenylyl cyclase activity by MOR agonists is strongly modulated by $\beta$ -arrestins

Activation of MORs by agonists can be manifested by a decrease in forskolin-stimulated AC activity in experimental conditions. Here, we assessed AC activity by measuring cAMP accumulation in HMY-1 cells and in HMY-1/ $\beta$ -Arr1<sup>(↓)</sup> or HMY-1/ $\beta$ -Arr2<sup>(↓)</sup> cells with downregulated  $\beta$ -arrestin 1 or  $\beta$ -arrestin 2, respectively (Fig. 4A). We were interested to see whether of siRNA knockdown of  $\beta$ -arrestins could influence the modulatory effects of opioid ligands on AC activity. We used DAMGO, morphine and endomorphin-2 at a concentration of 1  $\mu$ M in these experiments. In HMY-1 control cells we used scrambled siRNA as a control. Knockdown of  $\beta$ -arrestin 1 or  $\beta$ -arrestin 2 significantly suppressed forskolin-stimulated AC activity by about 65% or 30%, respectively (Fig. 4A). All MOR ligands decreased the production of cAMP in HMY-1 cells by about 28–42% and downregulation of  $\beta$ -arrestin isoforms differently affected the ability of MORs to inhibit forskolin-stimulated AC. Whereas the ability of activated-MORs to inhibit forskolin-stimulated AC activity was totally wiped out in cells lacking  $\beta$ -arrestin 1, knockdown of  $\beta$ -arrestin 2 did not change the ability of DAMGO, morphine and endomorphin-2 to inhibit the enzyme activity (Fig. 4A). To determine whether receptor-coupled Gi activity plays a role in the changes in AC activity seen with  $\beta$ -arrestin knockdown, the cells were pretreated with pertussis toxin (PTX) to eliminate all receptor-mediated Gi activation before measurement of AC activity. Intriguingly, knockdown of  $\beta$ -arrestin 2, in contrast to knockdown of  $\beta$ -arrestin 1, resulted

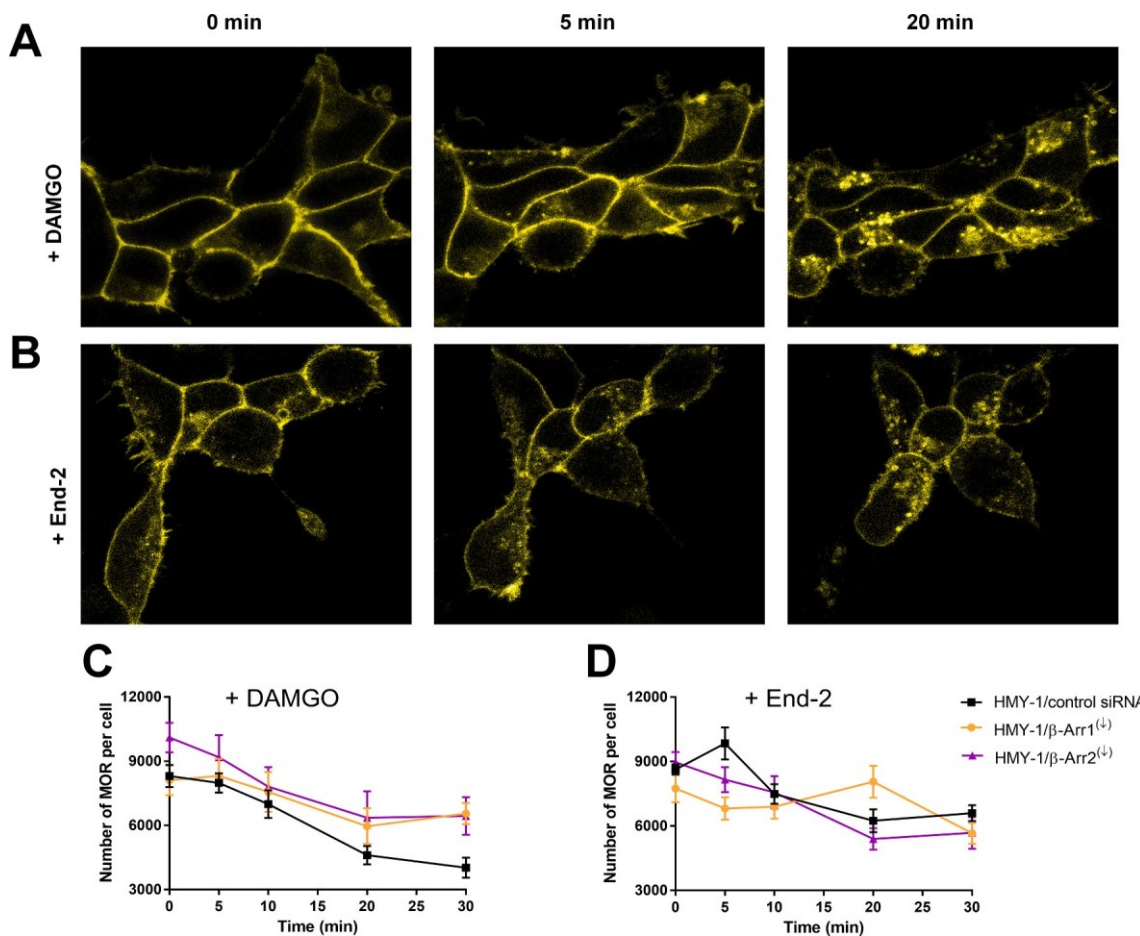


**Fig. 3.** Effect of  $\beta$ -arrestin knockdown on the internalization of MOR-YFP induced by MOR agonists. Confocal fluorescence images of HMY-1 cells incubated in the presence of DAMGO (A) or endomorphin-2 (End-2, B) at a final concentration of 1  $\mu$ M were taken at the beginning (0 min) and after 5 and 20 min. The time course of agonist-induced MORs internalization in HMY-1 cells and in cells with downregulated expression of  $\beta$ -arrestin 1 (HMY-1/ $\beta$ -Arr1 <sup>$\Delta$</sup> ) or  $\beta$ -arrestin 2 (HMY-1/ $\beta$ -Arr2 <sup>$\Delta$</sup> ) was monitored by radioligand binding assay using [<sup>3</sup>H]DAMGO as described in Methods. The cells were treated with DAMGO (C) or End-2 (B) for stated time intervals (0 - 30 min) and after washing they were incubated in the presence of [<sup>3</sup>H]DAMGO to determine the proportion of MORs associated with the plasma membrane. Data represent mean values  $\pm$  SEM of three independent experiments.

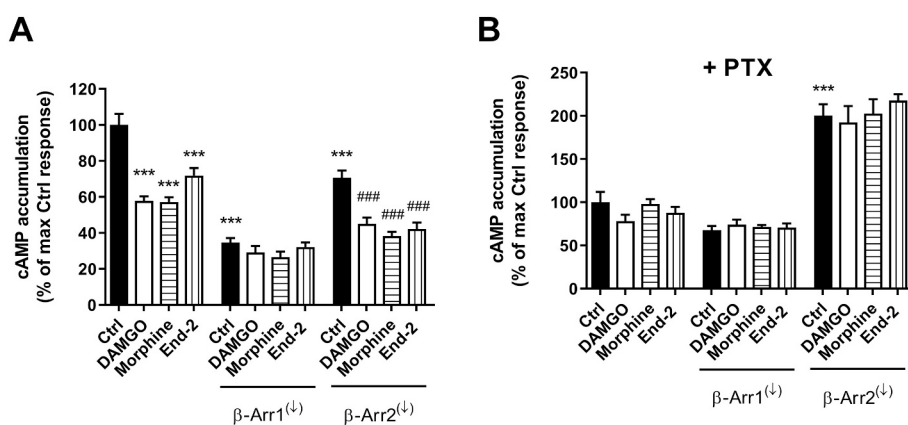


**Fig. 4.** Effect of  $\beta$ -arrestin knockdown and inactivation of  $G_{i\alpha}$  by PTX on the inhibition of forskolin-stimulated AC activity mediated by agonist-stimulated MORs. Cells were either not treated (A) or treated with 25 ng/ml PTX for 24 h before the experiment (B). HMY-1 cells and cells with down-regulated expression of  $\beta$ -arrestin 1 (HMY-1/ $\beta$ -Arr1 <sup>$\Delta$</sup> ) or  $\beta$ -arrestin 2 (HMY-1/ $\beta$ -Arr2 <sup>$\Delta$</sup> ) were incubated in the stimulation buffer supplemented with 0.5 mM IBMX and in the presence of DAMGO, morphine or End-2 at a final concentration of 1  $\mu$ M for 20 min at 37  $^{\circ}$ C. Afterwards, 2  $\mu$ M forskolin (Fsk) was added and after incubating for 45 min at 37  $^{\circ}$ C the accumulation of cAMP was determined using the HTRF cAMP-Gi kit from Cisbio. Results are expressed as mean  $\pm$  SEM of three independent experiments (\*\*\*)  $p < 0.001$  versus untreated Ctrl; ####  $p < 0.001$  versus respective Ctrl).

in significantly higher production of cAMP in PTX-treated cells (Fig. 4). This result indicates that receptor-coupled  $G_i$  activity plays a role in the changes in AC activity seen with  $\beta$ -arrestin 2 knockdown.

3.4. Adenylyl cyclase activity is modulated diversely by  $\beta$ -arrestin 1 and 2

AC can be activated directly by forskolin (a plant diterpene) or by the

stimulatory G proteins following agonist-stimulation of their cognate GPCRs. Here we investigated the effect of  $\beta$ -arrestin knockdown on cAMP production in HEK293 cells stimulated either by forskolin or isoprenaline, a potent  $\beta$ -adrenergic receptor agonist. The suppression of  $\beta$ -arrestin expression levels did not affect basal AC activity (data not shown). Interestingly, knockdown of  $\beta$ -arrestin 1 significantly reduced the ability of forskolin to activate AC; the maximal cAMP accumulation

dropped by about 55%. Contrarily, knockdown of  $\beta$ -arrestin 2 had an opposite effect; forskolin-stimulated cAMP production increased by about 39% in the presence of the highest forskolin concentration (Fig. 5A). When comparing dose–response curves of stimulation of AC by isoprenaline, no significant difference was observed between HEK293 cells and HEK293/ $\beta$ -Arr<sup>(↓)</sup> cells with downregulated  $\beta$ -arrestin 2. On the other hand, knockdown of  $\beta$ -arrestin 1 resulted in considerably lower accumulation of cAMP in cells stimulated by increased concentrations of isoprenaline; there was a drop of about 42% compared with control cells (Fig. 5B).

As a next step, we decided to test whether  $G_{\alpha s}$  may play a role in mediating the suppressing effect of  $\beta$ -arrestin 1 downregulation on AC activity. HEK293 cells and HEK293/ $\beta$ -Arr<sup>(↓)</sup> cells were transfected with  $G_{\alpha s}$  siRNA and cAMP production was measured upon stimulation with forskolin or isoprenaline. As expected, the silencing of  $G_{\alpha s}$  expression prevented activation of AC by isoprenaline (data not shown). The ability of forskolin to activate AC in HEK293/ $G_{\alpha s}$ <sup>(↓)</sup> cells with downregulated  $G_{\alpha s}$  was markedly reduced; cAMP accumulation induced by 50  $\mu$ M forskolin fell by 58% compared with control cells. Interestingly, simultaneous downregulation of  $G_{\alpha s}$  and  $\beta$ -arrestin 1 or  $G_{\alpha s}$  and  $\beta$ -arrestin 2 significantly suppressed AC activity even further; forskolin-stimulated cAMP production fell by about 79% in the presence of the highest forskolin concentration (Fig. 6). Potency ( $\log EC_{50}$ ) and efficacy ( $E_{max}$ ) values for forskolin and isoprenaline obtained from cAMP accumulation experiments are summarised in Table 1.

### 3.5. Activation of adenylyl cyclase promotes its interaction with $\beta$ -arrestins

Based on our previous observations regarding the impact of  $\beta$ -arrestin downregulation on AC activity, we were wondering if  $\beta$ -arrestin may interact with AC. To resolve this question, co-immunoprecipitation (Co-IP) experiments were performed using HEK293 cells transfected with a plasmid vector encoding  $\beta$ -arrestin 1-HA or  $\beta$ -arrestin 2-HA. The level of  $\beta$ -arrestin 1-HA or  $\beta$ -arrestin 2-HA protein expression was verified using western blot (data not shown). For Co-IP, the transfected cells were used either in an unaffected (resting) state or after activation with isoprenaline. We found that both  $\beta$ -arrestins can, to a certain extent, be associated with AC in a resting state, however  $\beta$ -arrestin 2-HA co-immunoprecipitated with AC less than  $\beta$ -arrestin 1-HA (Fig. 7). Interestingly, a relatively weak association of  $\beta$ -arrestins with AC in a basal state increased markedly after isoprenaline treatment, especially in the case of  $\beta$ -arrestin 1-HA (Fig. 7).

## 4. Discussion

$\beta$ -Arrestins can play different roles in cellular signaling processes. First of all, they are critically involved in modulating classical GPCR-dependent signal transduction, where they play a major role in

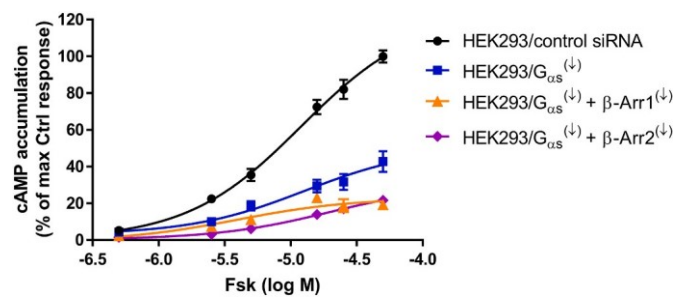


**Fig. 6.** Effect of  $G_{\alpha s}$ ,  $\beta$ -arrestin 1 and  $\beta$ -arrestin 2 knockdown on AC activity. HEK293 cells and cells with downregulated expression of  $G_{\alpha s}$  (HEK293/ $G_{\alpha s}$ <sup>(↓)</sup>) or  $G_{\alpha s}$  and  $\beta$ -arrestin 1 (HEK293/ $G_{\alpha s}$ <sup>(↓)</sup> +  $\beta$ -Arr1<sup>(↓)</sup>) or  $G_{\alpha s}$  and  $\beta$ -arrestin 2 (HEK293/ $G_{\alpha s}$ <sup>(↓)</sup> +  $\beta$ -Arr2<sup>(↓)</sup>) were treated with increasing concentrations of forskolin for 30 min at 37 °C. The accumulation of cAMP was determined using the HTRF cAMP-G $\gamma$  kit from Cisbio. Data represent mean values  $\pm$  SEM of three independent experiments.

receptor desensitization. Besides that  $\beta$ -arrestins function as scaffold proteins and may exercise their own signaling activity. However, not all the details of  $\beta$ -arrestin actions are fully understood. Our present study aimed at exploring the possible role of  $\beta$ -arrestin isoforms in lateral mobility of MORs in the plasma membrane and their presumed participation in the modulation of AC activity.

We used FRAP and line-scan FCS to determine the mobility of YFP-tagged MOR under different experimental conditions. It has been previously reported that different biased ligands of MORs can regulate the lateral mobility of MORs in the plasma membrane. Whereas DAMGO significantly increased MOR movement, endomorphin-2 had the opposite effect and morphine did not make any change [18]. Here, we observed that silencing of  $\beta$ -arrestin 1 and  $\beta$ -arrestin 2 significantly enhanced the rate of MOR diffusion and, simultaneously, the ability of endomorphin-2 and DAMGO to affect receptor mobility was abolished. On the other hand, the lateral mobility of MOR was not affected by morphine either in control HMY-1 cells or in cells lacking  $\beta$ -arrestin 1 or  $\beta$ -arrestin 2. These data suggest that  $\beta$ -arrestins are strongly implicated in the modulation of MOR diffusion in the plasma membrane upon stimulation by some agonists. To date, there are no clear indications that a disturbed interaction between of  $\beta$ -arrestins and GPCRs could affect the receptor mobility. Nevertheless, it can be inferred from a study of Kilpatrick et al. [26] that a mutation in the region of the NPY1 receptor which prevented  $\beta$ -arrestin recruitment was associated with a perceptible tendency towards increased lateral mobility of the NPY1 receptor and wiped out the ability of NPY to suppress the receptor movement. This is consistent with our observations and supports the notion that  $\beta$ -arrestins may influence GPCR motility. We did not observe any significant differences in the mobile fraction of MORs after knockdown of either of  $\beta$ -arrestin isoforms. However, the number of mobile receptors

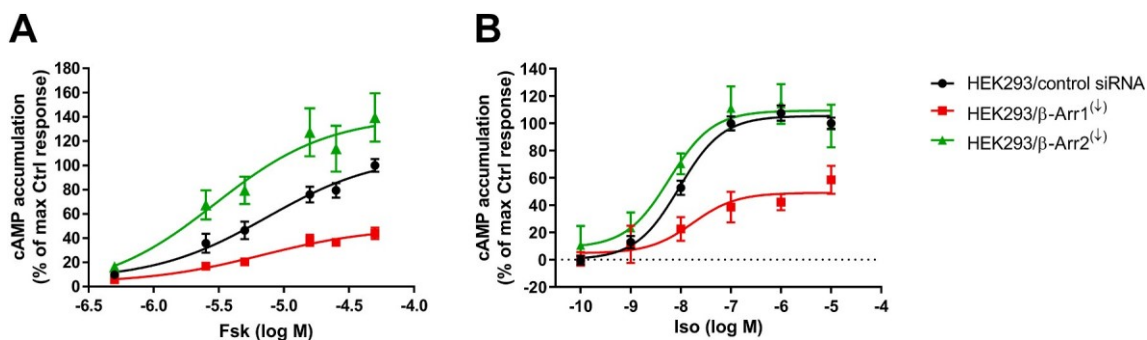


**Fig. 5.** Effect of  $\beta$ -arrestin knockdown on AC activity. HEK293 cells and cells with downregulated expression of  $\beta$ -arrestin 1 (HEK293/ $\beta$ -Arr1<sup>(↓)</sup>) or  $\beta$ -arrestin 2 (HEK293/ $\beta$ -Arr2<sup>(↓)</sup>) were treated with increasing concentrations of forskolin (Fsk) or isoprenaline (Iso) for 30 min at 37 °C. The accumulation of cAMP was determined using the HTRF cAMP-G $\gamma$  kit from Cisbio. Data represent mean values  $\pm$  SEM of three independent experiments.

**Table 1**  
Potency ( $\log EC_{50}$ ) and intrinsic efficacy ( $E_{max}$ ) of forskolin and isoprenaline.

	Forskolin						Isoprenaline		
	Control	$\beta$ -Arr1 <sup>(d)</sup>	$\beta$ -Arr2 <sup>(d)</sup>	$G_{05}$ <sup>(d)</sup>	$G_{05} + \beta$ -Arr1 <sup>(d)</sup>	$G_{05} + \beta$ -Arr2 <sup>(d)</sup>	Control	$\beta$ -Arr1 <sup>(d)</sup>	$\beta$ -Arr2 <sup>(d)</sup>
$\log EC_{50}$	$-4.9 \pm 0.1$	$-5.2 \pm 0.2$	$-5.4 \pm 0.2$	$-5.3 \pm 0.2$	$-5.4 \pm 0.2$	$-4.7 \pm 0.1$	$-7.9 \pm 0.1$	$-7.7 \pm 0.4$	$-8.2 \pm 0.1$
$E_{max}$ (%)	$120.8 \pm 5.1$	$49.2 \pm 7.6^{***}$	$147.8 \pm 15.3$	$42.1 \pm 10.4^{***}$	$19 \pm 2^{***}$	$31.2 \pm 5.8^{***}$	$103.5 \pm 1.9$	$49.4 \pm 8.4^{***}$	$109.8 \pm 6.1$

\*\*\*  $p < 0.001$  versus respective control.

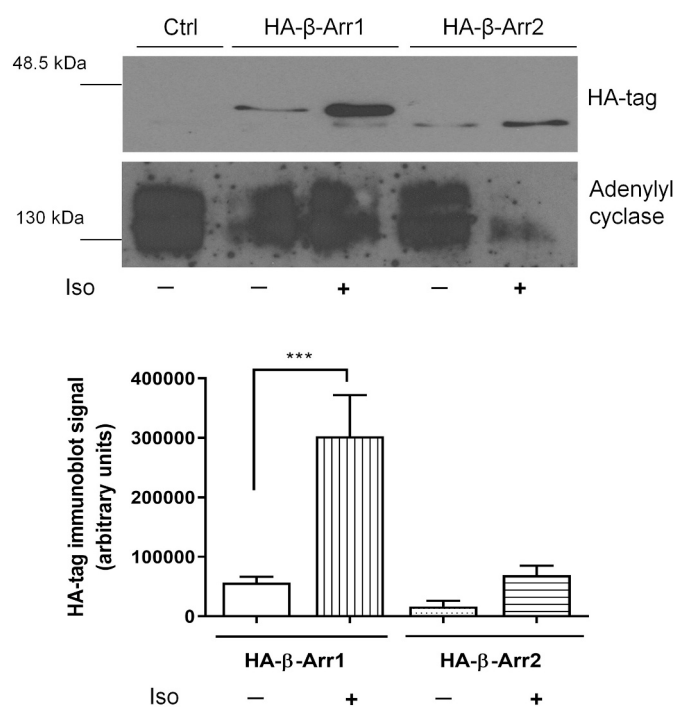


**Fig. 7.** Co-immunoprecipitation of  $\beta$ -arrestins with AC. Co-IP assay was performed using total homogenates from HEK293 cells (Ctrl) and from cells transiently transfected with HA-tagged  $\beta$ -arrestin 1 (HA- $\beta$ -Arr1) or HA-tagged  $\beta$ -arrestin 2 (HA- $\beta$ -Arr2) that were either untreated or treated with isoprenaline (Iso) for 10 min at 37 °C. Whole cell lysates were immunoprecipitated with anti-AC antibody. Subsequently, anti-AC and anti-HA antibodies were used for the immunolabeling reaction. (A) Representative Western blots showing the detection of AC and HA-tagged  $\beta$ -arrestins. (B) Relative densitometric analysis of HA-tagged  $\beta$ -arrestin immunoreactive bands. Data normalized to the weight of respective cells pellets are expressed as mean  $\pm$  SEM of three independent experiments (\*\*\*)  $p < 0.001$  versus untreated cells).

in the plasma membrane of HMY-1 cells with downregulated expression of  $\beta$ -arrestins somewhat decreased after stimulation with endomorphin-2 or DAMGO. This indicates that not only activation of the receptor but also interactions with  $\beta$ -arrestins and presumably other molecules, like heterotrimeric G-proteins, may affect receptor mobility. Similar observations were reported in several previous studies [23,27–30]. Our data from FRAP experiments have been corroborated by the results obtained by line-scan FCS. Although diffusion probed by FRAP during the recovery does not differ from the diffusion in equilibrium probed by FCS, imaging FCS techniques can apparently provide better and more stable diffusion coefficient values [25]. Importantly, both these methods revealed similar changes in the diffusion rates of MOR-YFP in our experimental conditions. Taken together, our results indicate that  $\beta$ -arrestins can strongly affect the lateral mobility of MORs in the plasma membrane. The lack of  $\beta$ -arrestin 1 or  $\beta$ -arrestin 2 was connected with increased MOR motility and altered sensitivity to modulation by agonists.

Both  $\beta$ -arrestin isoforms are known to play an important role in receptor desensitization, internalization, and intracellular trafficking.

GPCR endocytosis involves the coordinate interactions between receptor- $\beta$ -arrestin complexes and other endocytic proteins such as adaptor protein 2 (AP-2) and clathrin [31]. Interestingly, clathrin has been found to have a higher affinity for  $\beta$ -arrestin 2 than  $\beta$ -arrestin 1 [32] and AP-2 binds preferentially to  $\beta$ -arrestin 2 [33]. Moreover, some GPCRs apparently prefer to interact with  $\beta$ -arrestin 2 in the process of receptor internalization [34,35] and this isoform appears to be more efficient at translocating to the membrane upon agonist stimulation of several receptors [36]. Curiously, the interactions between  $\beta$ -arrestins and MORs have still not been adequately explored. So far there is only one study where Groer and colleagues revealed a higher affinity of MORs for  $\beta$ -arrestin 2 than for  $\beta$ -arrestin 1 [37]. This study defined DAMGO as a highly efficient ligand for the recruitment of  $\beta$ -arrestin 2. In the present experiments, we tested two different internalizing ligands of MORs, DAMGO and endomorphin-2. Morphine, a potent ligand of MORs, did not cause any internalization of these receptors. We noticed that endomorphin-2 was a bit less effective than DAMGO in eliciting MOR internalization. In contrast to DAMGO, there was an initial lag-phase of about 5 min before the evident internalization of MORs and significantly less receptors were removed from the plasma membrane in the presence of endomorphin-2 at the end of a 30-min incubation period. It is known that endomorphin-2 is biased towards  $\beta$ -arrestin and that DAMGO stabilizes a receptor conformation that preferentially activates G proteins [38]. We believe that the different ability of these two agonists to induce MOR internalization reflects their distinct bias properties. Accordingly, different internalization efficiency was also recently observed for other MOR agonists [39]. Selective silencing of the expression of  $\beta$ -arrestin 1 or  $\beta$ -arrestin 2 noticeably and to the same extent reduced maximal MOR internalization by DAMGO indicating that both these  $\beta$ -arrestin isoforms are recruited and utilized in the process of MOR sequestration and internalization upon binding of DAMGO. The recruitment of both  $\beta$ -arrestin 1 and 2 upon stimulation of MORs with DAMGO supports the notion about at least a partial interchangeability of  $\beta$ -arrestin isoforms in the internalization process of GPCRs [16,40]. On the other hand, dynamics of the internalization of MORs induced by endomorphin-2 was not significantly changed in cells with downregulated expression of  $\beta$ -arrestin 2 and knockdown of  $\beta$ -arrestin 1 led to the prevention of the internalization of MORs at 20 min by this ligand. This finding suggests preferential coupling between endomorphin-2-activated MOR and  $\beta$ -arrestin 1, which is in agreement with results obtained by Thompson et al. [41]. It can be assumed that biased ligands may stabilize distinct conformations of a receptor to enable discrete interactions with other signaling molecules, including  $\beta$ -arrestins.

The last part of this study was devoted to studying the presumed role of  $\beta$ -arrestins in modulation of AC activity under different experimental conditions. It is important to point out that these experiments were done with HMY-1 or HEK293 cells, which are closely related, but still not identical. This may explain partial discrepancies seen in some results regarding AC activity. The accumulation of cAMP in cells was monitored as a measure of AC function. Firstly, the inhibition of forskolin-stimulated AC was measured using three different ligands at a final concentration of 1  $\mu$ M. Intriguingly, knockdown of  $\beta$ -arrestin 1 markedly attenuated forskolin-stimulated AC activity and, in parallel, the ability of agonist-activated MORs to more suppress AC activity was abrogated. We did not find any significant difference between the inhibitory effects of endomorphin-2 and DAMGO or morphine in control cells. Similar findings were observed in cells with downregulated  $\beta$ -arrestin 2.

However, the lack of  $\beta$ -arrestin 2 did not have such profound implications for cAMP production. Forskolin-stimulated AC activity was somewhat reduced and the ability of all the three opioid agonists to inhibit the enzyme activity were not significantly changed. Pretreatment of cells with pertussis toxin, which is known to inactivate  $G_i\alpha$  proteins, hindered the ability of all three MOR ligands to inhibit AC activity in control cells as well as in cells with downregulated  $\beta$ -arrestin 1. On the other hand, pretreatment of cells lacking  $\beta$ -arrestin 2 with PTX resulted in enhanced accumulation of cAMP when compared to control cells. This result suggests that receptor-coupled  $G_i$  activity plays a role in the changes in AC activity seen with  $\beta$ -arrestin 2 knockdown and that  $\beta$ -arrestin 2 may function as a negative regulator of AC when  $G_i\alpha$  is inactivated. These results suggest that the extent of AC activation by forskolin as well as  $G_i$ -mediated MOR inhibition of the enzyme strongly depends on the presence of  $\beta$ -arrestins and that  $\beta$ -arrestin 1 and 2 play different roles in these phenomena.

A more detailed analysis of AC activity stimulated by forskolin and isoprenaline uncovered the distinct properties of  $\beta$ -arrestin isoforms with particular regard to modulation of the enzyme activity. Whereas forskolin-stimulated AC activity was significantly enhanced in cells lacking  $\beta$ -arrestin 2, it was markedly diminished in cells with downregulated expression of  $\beta$ -arrestin 1. Similar findings were noted for AC activity stimulated by the  $\beta$ -adrenergic receptor agonist isoprenaline, when the enzyme was activated through  $G_\alpha$ s. These findings imply that  $\beta$ -arrestin 1 is crucial for the effective functioning of AC while  $\beta$ -arrestin 2 rather dampens than amplifies the enzyme activity. These results partially correspond to some studies, where siRNA interference or knockout mice were used. Isoprenaline treatment of HEK293 cells with  $\beta$ -arrestin 2 siRNA resulted in significantly elevated cAMP accumulation and cells transfected with  $\beta$ -arrestin 1 siRNA exhibited a downward tendency in AC activity [34]. On the other hand, the use of mouse embryonic fibroblasts from  $\beta$ -arrestin 1 or  $\beta$ -arrestin 2 knockout mice led to the observation of increased cAMP accumulation after treatment with isoprenaline compared to wild type cells [16]. The partial discrepancy between these and our present results might be attributed to different experimental conditions, including cells, methods, ligand concentrations, and different incubation times. It has been previously disclosed that forskolin, a direct activator of AC, requires functional  $G_\alpha$ s for maximal activation of the enzyme [42,43]. In line with that we observed much lower production of cAMP in cells lacking  $G_\alpha$ s after activation with forskolin. Knockdown of  $\beta$ -arrestin 1 further deepened the drop in forskolin-stimulated AC activity under these conditions, suggesting that  $\beta$ -arrestin 1 may directly affect AC perhaps without participation of  $G_\alpha$ s. It is worth noting that  $\beta$ -arrestin 1 can directly interact with  $G_\alpha$ s and thus regulate its function [44]. However, this apparently does not prevent close communication between  $\beta$ -arrestins and AC. Our co-immunoprecipitation experiments provide evidence that  $\beta$ -arrestin 1 and AC may closely associate with each other, possibly by forming a complex that might contain some other proteins as well. Interestingly, the association of  $\beta$ -arrestin 1 with AC was profoundly enhanced by activation of AC by isoprenaline. This observation implies that  $G_\alpha$ s may possibly also participate in this interaction. Nevertheless, further research will be required to prove or disprove such a possibility. It seems that  $\beta$ -arrestin 2 may also interact with AC, but to a more limited extent. These findings are consistent with the observed distinct changes in cAMP accumulation due to selective silencing of  $\beta$ -arrestin expression.

Collectively, this study sheds new light on the similar and different capabilities of  $\beta$ -arrestin isoforms to modulate the behavior and functioning of selected key components of GPCR-mediated signal transduction system. Although we did not observe any significant differences in the ability of  $\beta$ -arrestin isoforms to influence the lateral mobility of MORs in the plasma membrane,  $\beta$ -arrestin 1 and  $\beta$ -arrestin 2 exhibited distinct modulatory effects on AC function. Moreover, we have demonstrated for the first time that  $\beta$ -arrestin 1, and partially  $\beta$ -arrestin 2, may interact with AC and that this interaction is strongly supported by the enzyme activation. These novel and exciting findings deserve further

investigation.

### CRedit authorship contribution statement

Lucie Hejnova: Methodology, Investigation, Formal analysis. Vendula Markova: Investigation, Data curation, Writing - original draft. Ales Benda: Methodology, Software. Jiri Novotny: Conceptualization, Supervision, Writing - review & editing. Barbora Melkes: Supervision, Methodology, Investigation, Writing - review & editing.

### Declaration of Competing Interest

The authors declare no competing interest.

### Acknowledgments

This work was supported by the Charles University, project GA UK No. 790217 and 1196120, and co-financed by the European Regional Development Fund and the state budget of the Czech Republic (CZ.1.05/4.1.00/16.0347). We acknowledge Imaging Methods Core Facility at BIOCEV, institution supported by the MEYS CR (Large RI Project LM2018129 Czech-BioImaging), for their support with obtaining Line-scan FCS data presented in this paper.

### Appendix A. Supplementary data

Supplementary data to this article can be found online at <https://doi.org/10.1016/j.cellsig.2021.110124>.

### References

- [1] K. Eichel, M. von Zastrow, Subcellular organization of GPCR signaling, *Trends Pharmacol. Sci.* 39 (2018) 200–208, <https://doi.org/10.1016/j.tips.2017.11.009>.
- [2] M. Zaccolo, A. Zerio, M.J. Lobo, Subcellular organization of the cAMP signaling pathway, *Pharmacol. Rev.* 73 (2021) 278–309, <https://doi.org/10.1124/pharmrev.120.000086>.
- [3] V.V. Gurevich, E.V. Gurevich, GPCR signaling regulation: the role of GRKs and arrestins, *Front. Pharmacol.* 10 (2019) 125, <https://doi.org/10.3389/fphar.2019.00125>.
- [4] S.A. Laporte, M.G.H. Scott,  $\beta$ -arrestins: multitask scaffolds orchestrating the where and when in cell signalling, *Methods Mol. Biol.* 2019 (1957) 9–55, [https://doi.org/10.1007/978-1-4939-9158-7\\_2](https://doi.org/10.1007/978-1-4939-9158-7_2).
- [5] D.S. Kang, X. Tian, J.L. Benovic, Role of  $\beta$ -arrestins and arrestin domain-containing proteins in G protein-coupled receptor trafficking, *Curr. Opin. Cell Biol.* 27 (2014) 63–71, <https://doi.org/10.1016/j.cob.2013.11.005>.
- [6] J.S. Smith, S. Rajagopal, The  $\beta$ -arrestins: multifunctional regulators of G protein-coupled receptors, *J. Biol. Chem.* 291 (2016) 8969–8977, <https://doi.org/10.1074/jbc.R115.713313>.
- [7] L. Ma, G. Pei, Beta-arrestin signaling and regulation of transcription, *J. Cell Sci.* 120 (2007) 213–218, <https://doi.org/10.1242/jcs.03338>.
- [8] J. van Gastel, J.O. Hendrickx, H. Leysen, P. Santos-Otte, L.M. Luttrell, B. Martin, S. Maudsley,  $\beta$ -arrestin based receptor signaling paradigms: potential therapeutic targets for complex age-related disorders, *Front. Pharmacol.* 9 (2018) 1369, <https://doi.org/10.3389/fphar.2018.01369>.
- [9] Z.J. Cheng, Q.M. Yu, Y.L. Wu, L. Ma, G. Pei, Selective interference of beta-arrestin 1 with kappa and delta but not mu opioid receptor/G protein coupling, *J. Biol. Chem.* 273 (1998) 24328–24333, <https://doi.org/10.1074/jbc.273.38.24328>.
- [10] L.M. Bohn, L.A. Dykstra, R.J. Lefkowitz, M.G. Caron, L.S. Barak, Relative opioid efficacy is determined by the complements of the G protein-coupled receptor desensitization machinery, *Mol. Pharmacol.* 66 (2004) 106–112, <https://doi.org/10.1124/mol.66.1.106>.
- [11] L.C. Sullivan, T.S. Chavera, R.J. Jamshidi, K.A. Berg, W.P. Clarke, Constitutive desensitization of opioid receptors in peripheral sensory neurons, *J. Pharmacol. Exp. Ther.* 359 (2016) 411–419, <https://doi.org/10.1124/jpet.116.232835>.
- [12] A. Gillis, A. Kliewer, E. Kelly, G. Henderson, M.J. Christie, S. Schulz, M. Canals, Critical assessment of G protein-biased agonism at the  $\mu$ -opioid receptor, *Trends Pharmacol. Sci.* 41 (2020) 947–959, <https://doi.org/10.1016/j.tips.2020.09.009>.
- [13] M.J. Clark, C.A. Furman, T.D. Gilson, J.R. Traynor, Comparison of the relative efficacy and potency of mu-opioid agonists to activate  $G_{\alpha(i/o)}$  proteins containing a pertussis toxin-insensitive mutation, *J. Pharmacol. Exp. Ther.* 317 (2006) 858–864, <https://doi.org/10.1124/jpet.105.096818>.
- [14] R. Sadana, C.W. Dessauer, Physiological roles for G protein-regulated adenylyl cyclase isoforms: insights from knockout and overexpression studies, *Neurosignals* 17 (2009) 5–22, <https://doi.org/10.1159/000166277>.
- [15] P.A. Insel, R.S. Ostrom, Forskolin as a tool for examining adenylyl cyclase expression, regulation, and G protein signaling, *Cell. Mol. Neurobiol.* 23 (2003) 305–314, <https://doi.org/10.1023/a:1023684503883>.

- [16] T.A. Kohout, F.S. Lin, S.J. Perry, D.A. Conner, R.J. Lefkowitz, beta-Arrestin 1 and 2 differentially regulate heptahelical receptor signaling and trafficking, *Proc. Natl. Acad. Sci. U. S. A.* 98 (2001) 1601–1606, <https://doi.org/10.1073/pnas.041608198>.
- [17] J.D. Violin, L.M. DiPilato, N. Yildirim, T.C. Elston, J. Zhang, R.J. Lefkowitz, beta2-adrenergic receptor signaling and desensitization elucidated by quantitative modeling of real time cAMP dynamics, *J. Biol. Chem.* 283 (2008) 2949–2961, <https://doi.org/10.1074/jbc.M707009200>.
- [18] B. Melkes, L. Hejnova, J. Novotny, Biased  $\mu$ -opioid receptor agonists diversely regulate lateral mobility and functional coupling of the receptor to its cognate G proteins, *Naunyn Schmiedeberg's Arch. Pharmacol.* 389 (2016) 1289–1300, <https://doi.org/10.1007/s00210-016-1293-8>.
- [19] M.A. Rapsomaniki, P. Kotsantis, I.-E. Symeonidou, N.-N. Giakoumakis, S. Taraviras, Z. Lygerou, easyFRAP: an interactive, easy-to-use tool for qualitative and quantitative analysis of FRAP data, *Bioinformatics* 28 (2012) 1800–1801, <https://doi.org/10.1093/bioinformatics/bts241>.
- [20] A. Benda, Y. Ma, K. Gaus, Self-calibrated line-scan STED-FCS to quantify lipid dynamics in model and cell membranes, *Biophys. J.* 108 (2015) 596–609, <https://doi.org/10.1016/j.bpj.2014.12.007>.
- [21] L.M. Luttrell, S.S. Ferguson, Y. Daaka, W.E. Miller, S. Maudsley, G.J. Della Rocca, F. Lin, H. Kawakatsu, K. Owada, D.K. Luttrell, M.G. Caron, R.J. Lefkowitz, Beta-arrestin-dependent formation of beta2 adrenergic receptor-Src protein kinase complexes, *Science* 283 (1999) 655–661, <https://doi.org/10.1126/science.283.5402.655>.
- [22] S. Ganguly, T.J. Pucadyil, A. Chattopadhyay, Actin cytoskeleton-dependent dynamics of the human serotonin1A receptor correlates with receptor signaling, *Biophys. J.* 95 (2008) 451–463, <https://doi.org/10.1529/biophysj.107.125732>.
- [23] R. Moravcova, B. Melkes, J. Novotny, TRH receptor mobility in the plasma membrane is strongly affected by agonist binding and by interaction with some cognate signaling proteins, *J. Recept. Signal Transduct. Res.* 38 (2018) 20–26, <https://doi.org/10.1080/10799893.2017.1398756>.
- [24] M. Yanagawa, M. Hiroshima, Y. Togashi, M. Abe, T. Yamashita, Y. Shichida, M. Murata, M. Ueda, Y. Sako, Single-molecule diffusion-based estimation of ligand effects on G protein-coupled receptors, *Sci. Signal.* 11 (2018), <https://doi.org/10.1126/scisignal.aao1917>.
- [25] R. Macha' n, Y.H. Foo, T. Wohland, On the equivalence of FCS and FRAP: simultaneous lipid membrane measurements, *Biophys. J.* 111 (2016) 152–161, <https://doi.org/10.1016/j.bpj.2016.06.001>.
- [26] L.E. Kilpatrick, S.J. Briddon, N.D. Holliday, Fluorescence correlation spectroscopy, combined with bimolecular fluorescence complementation, reveals the effects of  $\beta$ -arrestin complexes and endocytic targeting on the membrane mobility of neuropeptide Y receptors, *Biochim. Biophys. Acta* 2012 (1823) 1068–1081, <https://doi.org/10.1016/j.bbamcr.2012.03.002>.
- [27] L. C' ezanne, S. Lecat, B. Lagane, C. Millot, J.-Y. Vollmer, H. Matthes, J.-L. Galzi, A. Lopez, Dynamic confinement of NK2 receptors in the plasma membrane. Improved FRAP analysis and biological relevance, *J. Biol. Chem.* 279 (2004) 45057–45067, <https://doi.org/10.1074/jbc.M404811200>.
- [28] A. Sauli' ere-Nzeh Ndong, A.N. Sauli' ere-Nzeh, C. Millot, M. Corbani, S. Maz' eres, A. Lopez, L. Salom' e, Agonist-selective dynamic compartmentalization of human Mu opioid receptor as revealed by resolutive FRAP analysis, *J. Biol. Chem.* 285 (2010) 14514–14520, <https://doi.org/10.1074/jbc.M109.076695>.
- [29] U. Lalo, R.C. Allsopp, M.P. Mahaut-Smith, R.J. Evans, P2X1 receptor mobility and trafficking; regulation by receptor insertion and activation, *J. Neurochem.* 113 (2010) 1177–1187, <https://doi.org/10.1111/j.1471-4159.2010.06730.x>.
- [30] B. Melkes, V. Markova, L. Hejnova, J. Novotny,  $\beta$ -Arrestin 2 and ERK1/2 are important mediators engaged in close cooperation between TRPV1 and  $\mu$ -opioid receptors in the plasma membrane, *Int. J. Mol. Sci.* 21 (2020), <https://doi.org/10.3390/ijms21134626>.
- [31] Y.K. Peterson, L.M. Luttrell, The diverse roles of arrestin scaffolds in G protein-coupled receptor signaling, *Pharmacol. Rev.* 69 (2017) 256–297, <https://doi.org/10.1124/pr.116.013367>.
- [32] O.B. Goodman, J.G. Krupnick, F. Santini, V.V. Gurevich, R.B. Penn, A.W. Gagnon, J.H. Keen, J.L. Benovic,  $\beta$ -arrestin acts as a clathrin adaptor in endocytosis of the  $\beta$  2 -adrenergic receptor, *Nature* 383 (1996) 447–450, <https://doi.org/10.1038/383447a0>.
- [33] S.A. Laporte, R.H. Oakley, J. Zhang, J.A. Holt, S.S. Ferguson, M.G. Caron, L. S. Barak, The beta2-adrenergic receptor/betaarrestin complex recruits the clathrin adaptor AP-2 during endocytosis, *Proc. Natl. Acad. Sci. U. S. A.* 96 (1999) 3712–3717, <https://doi.org/10.1073/pnas.96.7.3712>.
- [34] S. Ahn, C.D. Nelson, T.R. Garrison, W.E. Miller, R.J. Lefkowitz, Desensitization, internalization, and signaling functions of  $\beta$ -arrestins demonstrated by RNA interference, *PNAS* 100 (2003) 1740–1744, <https://doi.org/10.1073/pnas.262789099>.
- [35] L.M. Luttrell, J. Wang, B. Plouffe, J.S. Smith, L. Yamani, S. Kaur, P.-Y. Jean-Charles, C. Gauthier, M.-H. Lee, B. Pani, J. Kim, S. Ahn, S. Rajagopal, E. Reiter, M. Bouvier, S.K. Shenoy, S.A. Laporte, H.A. Rockman, R.J. Lefkowitz, Manifold roles of  $\beta$ -arrestins in GPCR signaling elucidated with siRNA and CRISPR/Cas9, *Sci. Signal.* 11 (2018), <https://doi.org/10.1126/scisignal.aat7650>.
- [36] R.H. Oakley, S.A. Laporte, J.A. Holt, M.G. Caron, L.S. Barak, Differential affinities of visual arrestin, beta arrestin1, and beta arrestin2 for G protein-coupled receptors delineate two major classes of receptors, *J. Biol. Chem.* 275 (2000) 17201–17210, <https://doi.org/10.1074/jbc.M910348199>.
- [37] C.E. Groer, C.L. Schmid, A.M. Jaeger, L.M. Bohn, Agonist-directed interactions with specific  $\beta$ -arrestins determine  $\mu$ -opioid receptor trafficking, ubiquitination, and dephosphorylation, *J. Biol. Chem.* 286 (2011) 31731–31741, <https://doi.org/10.1074/jbc.M111.248310>.
- [38] G. Rivero, J. Llorente, J. McPherson, A. Cooke, S.J. Mundell, C.A. McArdle, E. M. Rosethorne, S.J. Charlton, C. Krasel, C.P. Bailey, G. Henderson, E. Kelly, Endomorphin-2: a biased agonist at the mu-opioid receptor, *Mol. Pharmacol.* 82 (2012) 178–188, <https://doi.org/10.1124/mol.112.078659>.
- [39] S. Manabe, K. Miyano, Y. Fujii, K. Ohshima, Y. Yoshida, M. Nonaka, M. Uzu, Y. Matsuoka, T. Sato, Y. Uezono, H. Morimatsu, Possible biased analgesic of hydromorphone through the G protein- $\beta$ -arrestin-mediated pathway: cAMP, & nbsp;Cell KeyTM, and receptor internalization analyses, *J. Pharmacol. Sci.* 140 (2019) 171–177, <https://doi.org/10.1016/j.jpsh.2019.06.005>.
- [40] S.M. DeWire, S. Ahn, R.J. Lefkowitz, S.K. Shenoy,  $\beta$ -arrestins and cell signaling, *Annu. Rev. Physiol.* 69 (2007) 483–510, <https://doi.org/10.1146/annurev.physiol.69.022405.154749>.
- [41] G.L. Thompson, J.R. Lane, T. Coudrat, P.M. Sexton, A. Christopoulos, M. Canals, Biased agonism of endogenous opioid peptides at the  $\mu$ -opioid receptor, *Mol. Pharmacol.* 88 (2015) 335–346, <https://doi.org/10.1124/mol.115.098848>.
- [42] D.A. Green, R.B. Clark, Direct evidence for the role of the coupling proteins in forskolin activation of adenylate cyclase, *J. Cyclic Nucleotide Res.* 8 (1982) 337–346.
- [43] M. Chen-Goodspeed, A.N. Lukan, C.W. Dessauer, Modeling of Galpha(s) and Galpha(i) regulation of human type V and VI adenylyl cyclase, *J. Biol. Chem.* 280 (2005) 1808–1816, <https://doi.org/10.1074/jbc.M409172200>.
- [44] B. Li, C. Wang, Z. Zhou, J. Zhao, G. Pei,  $\beta$ -Arrestin-1 directly interacts with Gas and regulates its function, *FEBS Lett.* 587 (2013) 410–416, <https://doi.org/10.1016/j.febslet.2013.01.027>.



Article

# $\beta$ -Arrestin 2 and ERK1/2 Are Important Mediators Engaged in Close Cooperation between TRPV1 and $\mu$ -Opioid Receptors in the Plasma Membrane

Barbora Melkes, Vendula Markova, Lucie Hejnova and Jiri Novotny \*

Department of Physiology, Faculty of Science, Charles University, 128 00 Prague, Czech Republic; barbora.melkes@natur.cuni.cz (B.M.); vendula.markova@natur.cuni.cz (V.M.); lucie.hejnova@natur.cuni.cz (L.H.)

\* Correspondence: jiri.novotny@natur.cuni.cz; Tel.: +240-22-195-1760

Received: 29 May 2020; Accepted: 28 June 2020; Published: 29 June 2020



**Abstract:** The interactions between TRPV1 and  $\mu$ -opioid receptors (MOR) have recently attracted much attention because these two receptors play important roles in pain pathways and can apparently modulate each other's functioning. However, the knowledge about signaling interactions and crosstalk between these two receptors is still limited. In this study, we investigated the mutual interactions between MOR and TRPV1 shortly after their activation in HEK293 cells expressing these two receptors. After activation of one receptor we observed significant changes in the other receptor's lateral mobility and vice versa. However, the changes in receptor movement within the plasma membrane were not connected with activation of the other receptor. We also observed that plasma membrane  $\beta$ -arrestin 2 levels were altered after treatment with agonists of both these receptors. Knockdown of  $\beta$ -arrestin 2 blocked all changes in the lateral mobility of both receptors. Furthermore, we found that  $\beta$ -arrestin 2 can play an important role in modulating the effectiveness of ERK1/2 phosphorylation after activation of MOR in the presence of TRPV1. These data suggest that  $\beta$ -arrestin 2 and ERK1/2 are important mediators between these two receptors and their signaling pathways. Collectively, MOR and TRPV1 can mutually affect each other's behavior and  $\beta$ -arrestin 2 apparently plays a key role in the bidirectional crosstalk between these two receptors in the plasma membrane.

**Keywords:**  $\mu$ -opioid receptor; TRPV1;  $\beta$ -arrestin 2; ERK1/2; biased signaling; receptor lateral mobility

## 1. Introduction

Large numbers of studies conducted over the previous decades have increased knowledge of pain mechanisms at both the cellular and molecular level. Several membrane-bound receptors and ion channels have been found to play a key role in the transmission or attenuation of painful stimuli. Among them, the  $\mu$ -opioid receptor (MOR) has attracted great attention as the primary molecular target of opioid drugs, a group of most effective analgesics [1,2]. MOR belongs to the family of G protein-coupled receptors (GPCRs). MOR is linked to the inhibitory G proteins, whose major signaling pathway leads to inhibition of adenylyl cyclase or modulation of mitogen activated protein kinases (MAPKs). The properties of these receptors and their signaling systems have been extensively studied not only in connection with nociception but also with a potential risk of tolerance and dependence associated with long-term use or abuse of opioids [3–5]. Interestingly, it has been observed that MOR-initiated signaling can be modulated by other GPCRs or some ion channels. In the case of antinociception, communication between the MOR and TRPV1 (transient receptor potential vanilloid 1) receptors appears particularly noteworthy [6,7].

TRPV1 receptors, which play a central role in thermal nociception and inflammation-induced hyperalgesia, belong to the large superfamily of TRP ion channels [8]. These are ligand-driven, non-selective cation channels that are present at low levels in different types of cells and tissues but are primarily expressed in the posterior spinal neurons and trigeminal ganglia [9]. TRPV1 receptors are considered to be important molecular integrators of nociceptive stimuli because they respond not only to elevated temperature but also to reduced pH, vanilloids (e.g., capsaicin), and other pain-inducing substances (e.g., arachidonic acid metabolites). Furthermore, these receptors serve as the final target structure of intracellular signaling pathways triggered by inflammatory mediators, thereby potentiating their activity and contributing to elevated hyperexcitability and nociception [10]. Thus, the function of TRPV1 receptors can be regulated through their direct activation by “external” pain stimuli or through “intrinsic” sensitization induced by intracellular signaling cascades that are linked to GPCRs or receptor tyrosine kinases (RTKs). The sensitization of TRPV1 receptors is based on their post-translational modifications, such as protein kinase A (PKA)- and protein kinase C (PKC)-mediated phosphorylation [11].

Previous studies have demonstrated natural co-expression of MOR and TRPV1 receptors in different regions of the central nervous system and pointed to possible functional interactions between these receptors [7,12]. In the recent past, Bao et al. [13] have noticed that MOR and TRPV1 receptor agonists may have conflicting effects on antinociception, tolerance, and dependence. It has been repeatedly observed that administration of morphine can induce antinociceptive effects by modulating the activity of TRPV1 receptors. As indicated above, TRPV1 receptors can be activated in a variety of ways. However, the potential specific effects of MOR agonists on TRPV1 receptors and vice versa have not yet been fully explored.

Recent evidence suggests that functional communication between MOR and TRPV1 receptors is bilateral and highly dependent on specific conditions; the mechanism and duration of activation of these receptors seem particularly important. However, many intriguing questions regarding MOR–TRPV1 interactions, crosstalk between their signaling pathways, and respective feedback loops still remain unresolved. Therefore, in the present study we set out to investigate behavior and functional properties of these receptors and their signaling pathways in defined *in vitro* conditions and examine the role of key components of both these important cellular signaling systems in their mutual communication (Figure 1).

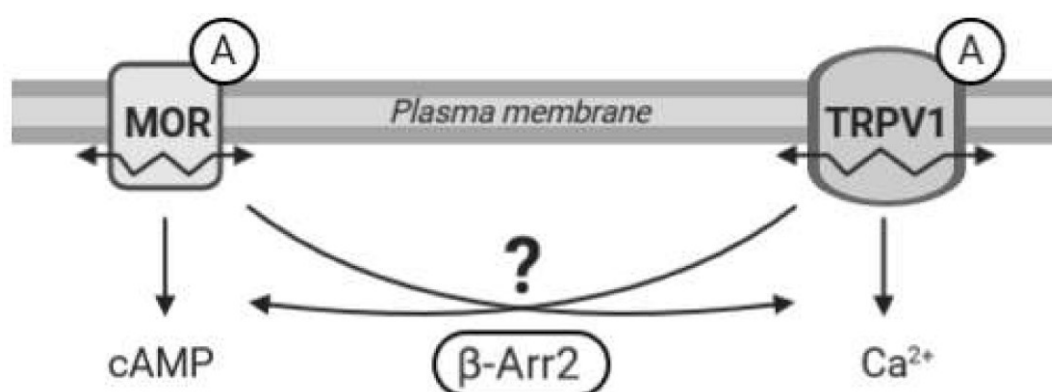


**Figure 1.** Working hypothesis. The diagram illustrates a presumed crosstalk between the  $\mu$ -opioid receptor (MOR) and TRPV1 following stimulation by agonists (A).  $\beta$ -Arrestin 2 ( $\beta$ -Arr2) plays an important role in signal transduction pathways initiated by MOR and TRPV1. We hypothesize that  $\beta$ -arrestin 2 may also participate in mutual communication between these two receptors. We speculate that activation of one receptor may affect functioning and mobility ( ) in the plasma membrane of the other receptor and that  $\beta$ -arrestin 2 could mediate these interactions.

## 2. Results

### 2.1. Transient Transfection of HMY-1 Cells with TRPV1-CFP

HMY-1 cells stably expressing MOR-YFP fusion construct [14] were transiently transfected with TRPV1-CFP fusion construct as described in Section 4. The transfection efficiency of TRPV1-CFP into HMY-1 cells was >60%. The expression and plasma membrane localization of TRPV1 and MOR is shown in Figure 2A,B, respectively. This figure displays representative TIRF images of the bottom membrane of HMY-1/TRPV1 cells taken by a super-resolution microscope (Zeiss Elyra).

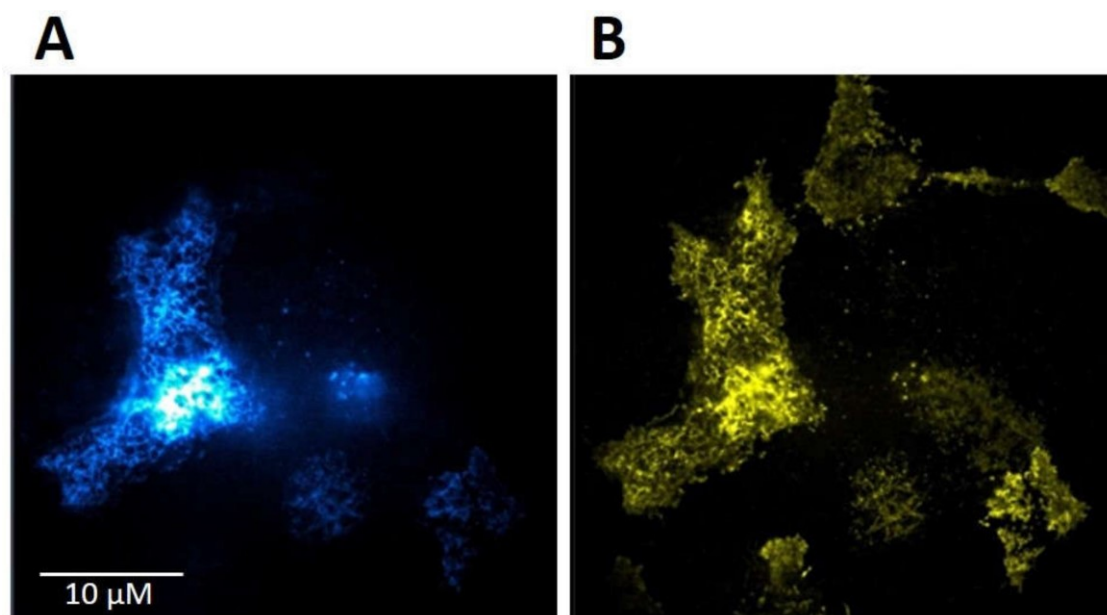


**Figure 2.** Expression of TRPV1 and MOR in HMY-1/TRPV1 cells. HMY-1 cells were transiently transfected with a construct expressing TRPV1-CFP as described in Section 4. Representative images of a group of HMY-1/TRPV1 cells (focus on the bottom cell membrane) demonstrate the distribution of the fluorescence signal corresponding to TRPV1-CFP (A) and MOR-YFP (B) in the plasma membrane. Both these photographs were taken using the TIRF mode of super-resolution microscope Zeiss Elyra.

### 2.2. Activation of TRPV1 Affects MOR Mobility at the Cell Surface

First, we measured the diffusion coefficients of MOR under different experimental conditions. HMY-1 cells were seeded in a glass bottom chamber, transiently transfected with TRPV1-CFP construct and after 24-h incubation ligands of interest were added. In the case of the MOR agonist endomorphin-2, we observed changes similar to those seen in HMY-1 cells without TRPV1-CFP [14], i.e., a decrease in the rate of receptor diffusion (Figure 3A). On the other hand, the diffusion coefficient of MOR increased at least twofold after treatment of the cells with the TRPV1 agonist capsaicin (control,  $D = 0.358 \pm 0.036 \mu\text{m}^2/\text{s}$ ; capsaicin,  $D = 0.978 \pm 0.077 \mu\text{m}^2/\text{s}$ ). To check the specific effect of agonists, some cells were treated with antagonist before adding the agonists. Pretreatment of the cells with naloxone or capsazepine completely blocked the effects of the MOR agonist endomorphin-2 or TRPV1 agonist capsaicin, respectively.

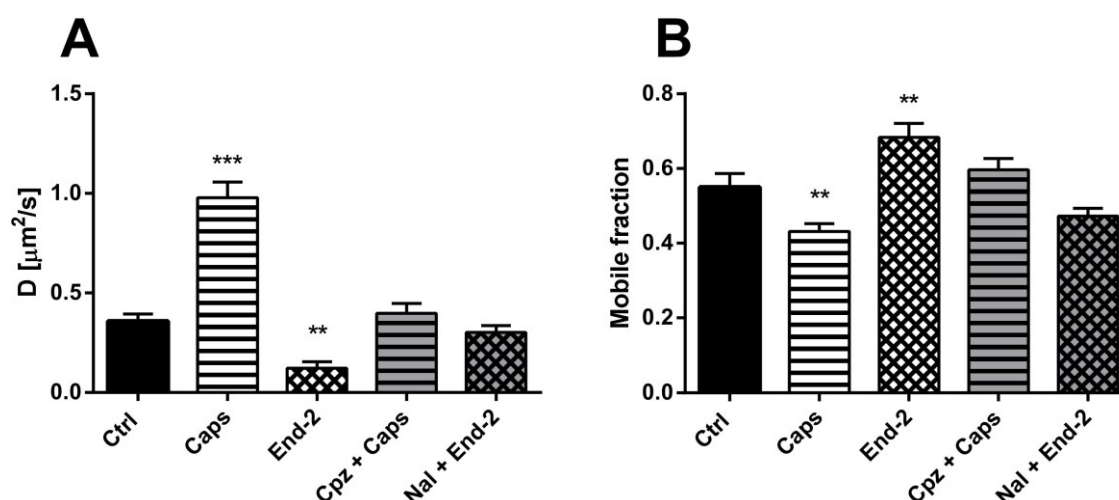


**Figure 3.** Effect of different ligands on the lateral mobility of MOR in the plasma membrane of HMY-1/TRPV1 cells. The diffusion coefficients (A) and the mobile fractions (B) of MOR were obtained from fluorescent recovery after photobleaching (FRAP) measurements. The cells plated in a glass bottom chamber were treated with capsaicin (Caps, 0.5  $\mu\text{M}$ ) or endomorphin-2 (End-2, 1  $\mu\text{M}$ ) for 5 min before measurements. In some cases, the cells were incubated in the presence of the TRPV antagonist capsazepine (Cpz) or the MOR antagonist naloxone (Nal) (both 10  $\mu\text{M}$ ) for 10 min prior to addition of the agonists. FRAP experiments were performed on the bottom cell membrane using a Zeiss LSM 880 confocal microscope. The data were collected from three independent experiments, at least 50 cells in each group. Results are expressed as means  $\pm$  S.E.M. Asterisks denote significant differences between control (Ctrl) and different drug treatment groups (\*\*  $p < 0.01$ , \*\*\*  $p < 0.001$  compared to corresponding control).

Next, we determined the proportion of mobile and immobile receptors in the plasma membrane after activation of both MOR and TRPV1 with their cognate agonists. Whereas the mobile fraction of MOR significantly increased after treatment of HMY-1/TRPV1 cells with endomorphin-2, this fraction markedly decreased in the presence of capsaicin (Figure 3B). The effects of either agonist were prevented when the respective antagonists (naloxone and capsazepine) were added to cell culture media prior to each agonist.

### 2.3. Activation of MOR Affects TRPV1 Mobility at the Cell Surface

The diffusion of unactivated TRPV1 ( $D = 0.75 \pm 0.07 \mu\text{m}^2/\text{s}$ ) was higher than the diffusion of unactivated MOR ( $D = 0.36 \pm 0.03 \mu\text{m}^2/\text{s}$ ) in cells expressing both these receptors. After activation of TRPV1 with capsaicin, the diffusion coefficient of this receptor increased more than two times ( $D = 1.590 \pm 0.136 \mu\text{m}^2/\text{s}$ ), compared to the control vehicle-treated cells ( $D = 0.73 \pm 0.09 \mu\text{m}^2/\text{s}$ ). Moreover, activation of MOR with endomorphin-2 also increased the diffusion coefficient of TRPV1 ( $D = 1.150 \pm 0.121 \mu\text{m}^2/\text{s}$ ), but less than capsaicin (Figure 4A). Importantly, pretreatment of the cells with naloxone or capsazepine prevented the agonist-induced changes in the receptor diffusion.

Treatment of HMY-1/TRPV1 cells with both capsaicin and endomorphin-2 changed the proportion of mobile and immobile TRPV1 in the plasma membrane. Whereas capsaicin reduced the mobile fraction of TRPV1, endomorphin-2 markedly increased the mobile fraction of TRPV1 (Figure 4B). Pretreatment of the cells with naloxone or capsazepine before adding endomorphin-2 or capsaicin prevented the effects of both these agonists.

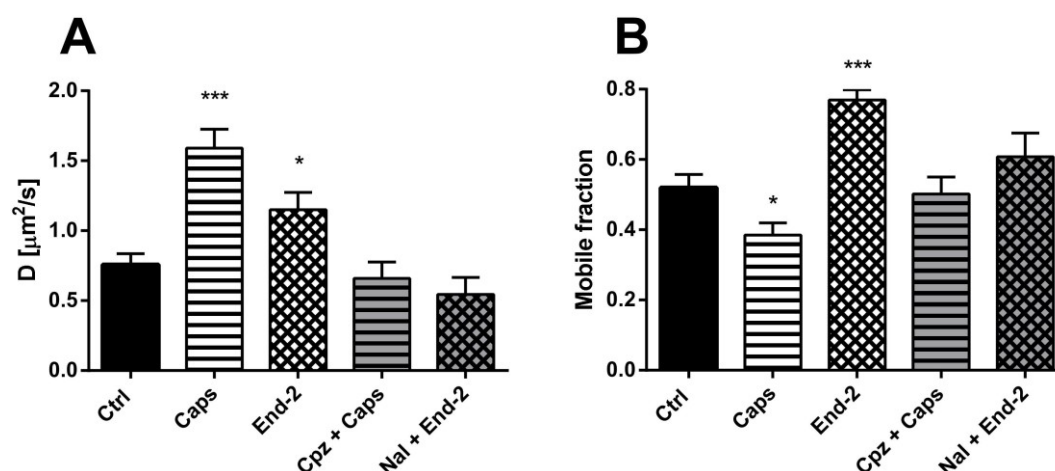


**Figure 4.** Effect of different ligands on the lateral mobility of TRPV1 in the plasma membrane of HMY-1/TRPV1 cells. The diffusion coefficients (A) and the mobile fractions (B) of MOR were obtained from FRAP measurements. The cells plated in a glass bottom chamber were treated with capsaicin (Caps, 0.5  $\mu\text{M}$ ) or endomorphin-2 (End-2, 1  $\mu\text{M}$ ) for 5 min before measurements. In some cases, the cells were incubated in the presence of the TRPV antagonist capsazepine (Cpz) or the MOR antagonist naloxone (both 10  $\mu\text{M}$ ) for 10 min prior to addition of the agonists. FRAP experiments were performed on the bottom cell membrane using a Zeiss LSM 880 confocal microscope. The data were collected from three independent experiments, at least 50 cells in each group. Results are expressed as means  $\pm$  S.E.M. Asterisks denote significant differences between control (Ctrl) and different drug treatment groups (\*  $p < 0.05$ , \*\*\*  $p < 0.001$  compared to corresponding control).

#### 2.4. Knockdown of $\beta$ -Arrestin 2 Prevents Activation-Induced Changes in the Mobility of Both TRPV1 and MOR

In order to explore the possible role of  $\beta$ -arrestin 2 in modulating the mobility of MOR and TRPV1 in the plasma membrane, the receptor diffusion was monitored in HMY-1/TRPV1 cells after knockdown of  $\beta$ -arrestin 2. The efficacy of siRNA-mediated  $\beta$ -arrestin 2 knockdown was confirmed by Western blotting. This analysis indicated that the expression of  $\beta$ -arrestin 2 was downregulated by about 90% in cells transfected with  $\beta$ -arrestin 2 siRNA. Interestingly, knockdown of  $\beta$ -arrestin strongly affected receptor diffusibility and limited the modulatory effects of agonists on receptor movement.

In the case of MOR, knockdown of  $\beta$ -arrestin 2 somewhat decreased (by about 16%) the lateral mobility of unactivated MOR (Figure 5A). Moreover, this intervention markedly attenuated the ability of capsaicin and endomorphin-2 to affect the rate of diffusion of MOR. Whereas capsaicin increased the rate of MOR diffusion by 42%, endomorphin-2 did not change the receptor movement under these conditions. Interestingly, the proportion of mobile MOR significantly increased (by about 18%) after  $\beta$ -arrestin 2 knockdown (Figure 5B). Capsaicin reduced the MOR mobile fraction (by 22%) in HMY-1/TRPV1 cells with suppressed expression of  $\beta$ -arrestin 2 to a similar extent as in the cells carrying a normal level of  $\beta$ -arrestin 2 (decrease by about 21%). Addition of endomorphin-2 to HMY-1/TRPV1 cells after  $\beta$ -arrestin 2 knockdown reduced the MOR mobile fraction by about 17%.  $\beta$ -Arrestin 2 knockdown substantially decreased (by about 47%) the lateral mobility of TRPV1 and its rate of diffusion was increased to the same extent (by about 25%) by the addition of capsaicin or endomorphin-2 (Figure 5C). The fraction of mobile receptors was significantly increased after knockdown of  $\beta$ -arrestin 2 (by about 25%) and the addition of capsaicin or endomorphin-2 reduced the proportion of mobile TRPV1 back to the control level (Figure 5D). This was in contrast to normal MY-1/TRPV1 cells, where endomorphin-2 significantly increased (by about 20–30%) the proportion of mobile MOR and TRPV1.

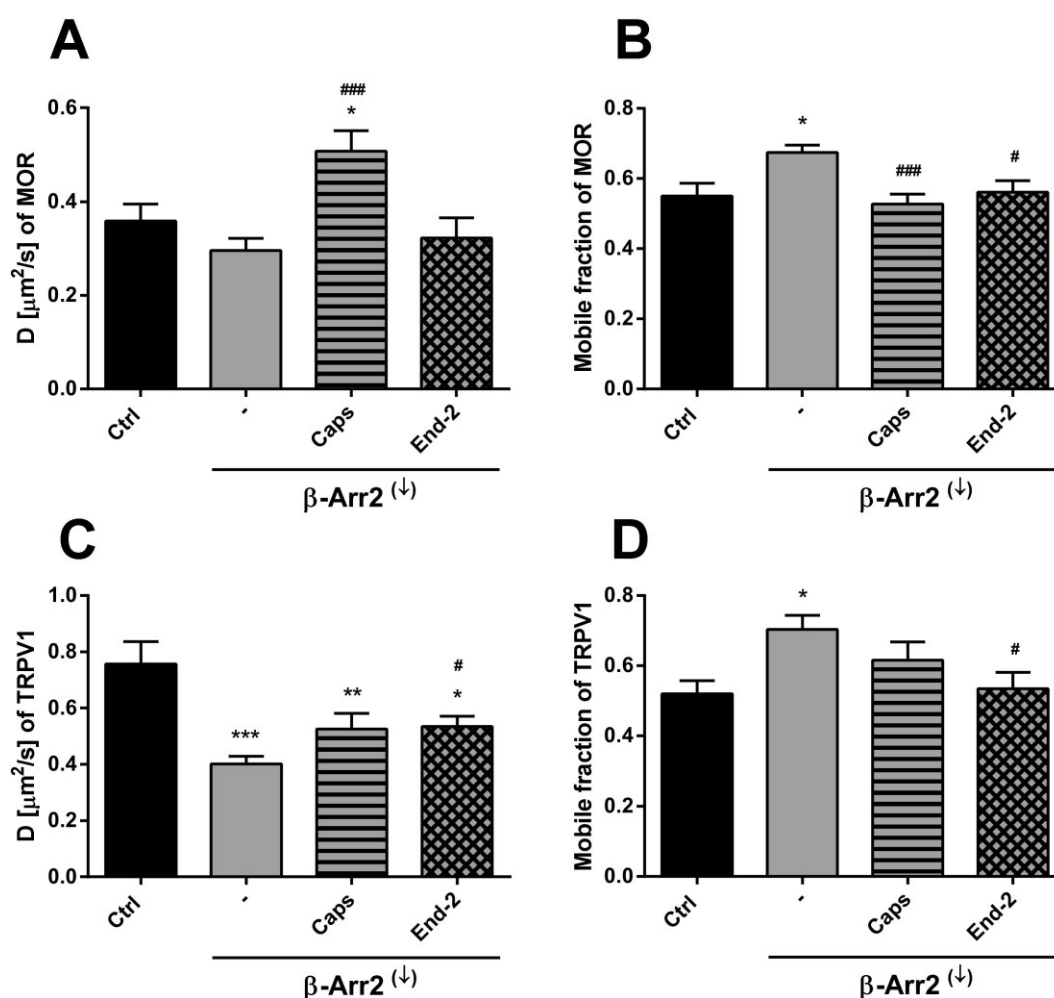


**Figure 5.** Effect of  $\beta$ -arrestin 2 knockdown on the ability of capsaicin and endomorphin-2 to affect the lateral mobility of MOR and TRPV1 in the plasma membrane of HMY-1/TRPV1 cells. The diffusion coefficients (A,C) and the mobile fractions (B,D) of TRPV1 (upper panel) and MOR (lower panel) were obtained from FRAP measurements. The knockdown of  $\beta$ -arrestin 2 ( $\beta$ -Arr2 $\downarrow$ ) was performed 24 h before addition of the ligands. The cells plated in a glass bottom chamber were treated with capsaicin (Caps, 0.5  $\mu$ M) or endomorphin-2 (End-2, 1  $\mu$ M) for 5 min before measurements. FRAP experiments were performed on the bottom cell membrane using a Zeiss LSM 880 confocal microscope. The data were collected from three independent experiments, at least 50 cells in each group. Results are expressed as means  $\pm$  S.E.M. Asterisks or hashes denote significant differences between control (Ctrl) or untreated (-)  $\beta$ -Arr2 $\downarrow$  cells and different drug treatment groups (\*  $p < 0.05$ , \*\*  $p < 0.01$ , \*\*\*  $p < 0.001$  compared to corresponding control; #  $p < 0.05$ , ###  $p < 0.001$  compared to corresponding  $\beta$ -Arr2 $\downarrow$  (-)).

### 2.5. Functional Studies of MOR and TRPV1 Signaling

In this set of experiments, we examined agonist-induced  $\text{Ca}^{2+}$  responses and inhibition of adenylyl cyclase (AC) activity in HMY-1 and HMY-1/TRPV1 cells. We found that the TRPV1 agonist capsaicin was able to evoke a dose-dependent  $\text{Ca}^{2+}$  influx only in HMY-1/TRPV1 cells (Figure 6A). No such response was observed on HMY-1 cells. The MOR agonist endomorphine-2 did not elicit any detectable  $\text{Ca}^{2+}$  responses at any concentration. The ability of receptor agonists to affect forskolin-stimulated AC was determined using the HTRF assay (Cisbio Bioassays). Whereas capsaicin did not change AC activity either in HMY-1 or HMY-1/TRPV1, endomorphin-2 inhibited the enzyme activity in both these cell lines to a similar extent (Figure 6B).

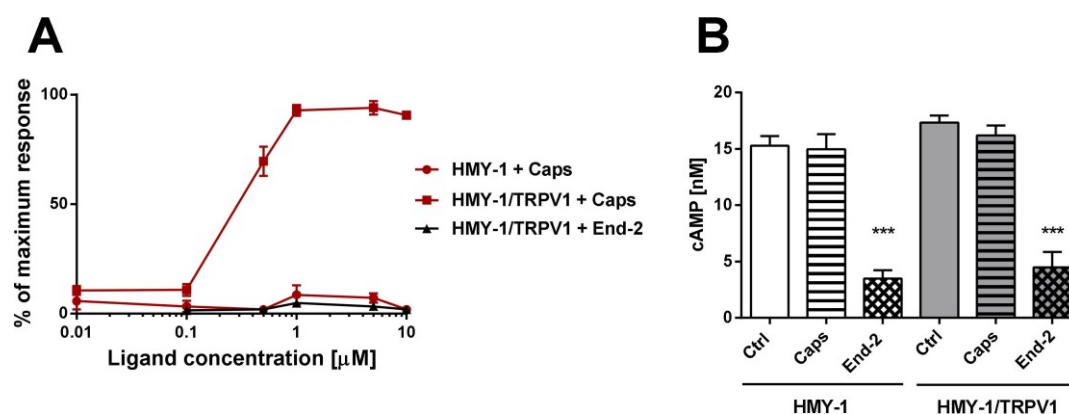


**Figure 6.** Functional studies of TRPV1- and MOR-mediated signaling. (A) The effect of increasing concentrations of capsaicin (Caps) and endomorphin-2 (End-2) on intracellular levels of calcium in HMY-1 and HMY-1/TRPV1 cells was determined using endpoint calcium assay described in Section 4. The graph shows calcium response to agonist stimulation expressed as percentage of the maximum response. (B) The effect of capsaicin and endomorphin-2 (both 1  $\mu$ M) on cAMP production in HMY-1 and HMY-1/TRPV1 cells incubated in the presence of forskolin was determined using TRF assay described in Section 4. Results are expressed as means  $\pm$  S.E.M. (\*\*\*)  $p \leq 0.001$  compared to corresponding control).

#### 2.6. Activation of TRPV1 and MOR Alters the Plasma Membrane Localization of $\beta$ -Arrestin 2

We were interested to determine whether stimulation of HMY-1 and HMY-1/TRPV1 affected the association of  $\beta$ -arrestin 2 with the plasma membrane. After incubating the cells for 5 min in the presence of capsaicin or endomorphin-2, the relative level of  $\beta$ -arrestin 2 in the plasma membrane fraction was assessed by immunoblot analysis. Both capsaicin and endomorphin-2 markedly reduced (by about 50%) the content of  $\beta$ -arrestin 2 in samples of plasma membranes from HMY-1/TRPV1 cells (Figure 7A). There was no such change in the plasma membrane distribution of  $\beta$ -arrestin 2 after treatment of HMY-1 cells by these agonists.

Then, we investigated the localization of  $\beta$ -arrestin 2 at the plasma membrane using TIRF microscopy. HMY-1 and HMY-1/TRPV1 cells stained with antibody against  $\beta$ -arrestin 2 and Alexa Fluor 594-conjugated secondary antibody were visualized with Zeiss Elyra SP.1 nanoscope (Figure 7B). These experiments indicated that transfection of HMY-1 cells with TRPV1 did not change the level of  $\beta$ -arrestin 2 associated with the plasma membrane (Figure 7C). Interestingly, pretreatment of HMY-1/TRPV1 cells, but not HMY-1 cells, with capsaicin and endomorphin-2 reduced the plasma membrane localization of  $\beta$ -arrestin 2.

#### 2.7. Crosstalk between TRPV1 and MOR Signaling Is Driven via the MAPK ERK1/2 Pathway

It seems obvious that  $\beta$ -arrestin 2 can play an important role in mediating crosstalk between TRPV1 and MOR. To decipher the potential involvement of post-receptor signaling pathways in cross-communication between both these receptors, we monitored protein phosphorylation changes of key components of the MAPK signaling cascades in response to stimulation of HEK293/TRPV1, HMY-1/TRPV1, and HMY-1 cells by capsaicin and endomorphin-2. Phospho- and total protein levels of ERK1/2, p38 and JNK were assessed by immunoblotting (Figure 8). Capsaicin remarkably increased phosphorylation of ERK1/2 in cells expressing TRPV1 (HEK293/TRPV1 and HMY-1/TRPV1). No significant change occurred in HMY-1 cells. Endomorphin-2 increased phosphorylation of ERK1/2 in cells expressing MOR (HMY-1 and HMY-1/TRPV1). Intriguingly, a much greater elevation of ERK1/2 phosphorylation was found in cells expressing both MOR and TRPV1 (Figure 8A). We performed yet another set of experiments on cells with reduced expression of  $\beta$ -arrestin 2. Knockdown of  $\beta$ -arrestin 2 did not affect capsaicin-induced phosphorylation of ERK1/2, but strongly attenuated the ability of endomorphin-2 to increase phosphorylation of ERK1/2 in the cells expressing both MOR and TRPV1

(Figure 8B). The phosphorylation levels of the other two MAP kinases, p38 and JNK, were not changed in either cell line after treatment with both agonists (Figure 8C,D).

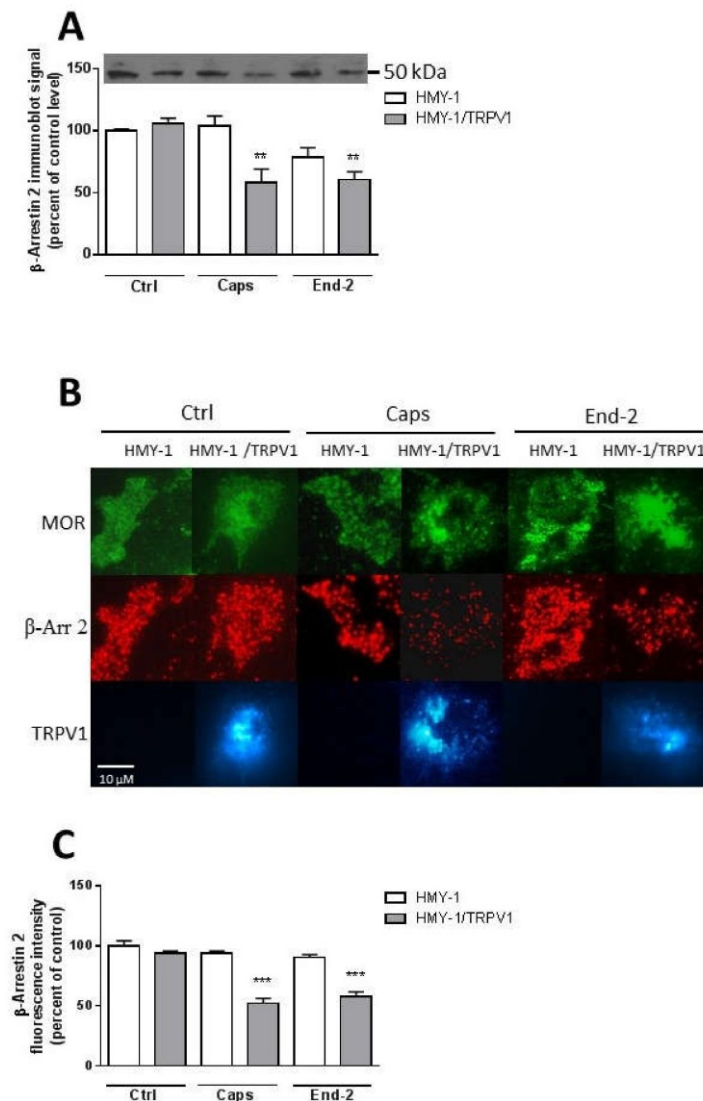


**Figure 7.** Effect of capsaicin and endomorphin-2 on the association of  $\beta$ -arrestin 2 with the plasma membrane. **(A)** Immunoblot analysis of  $\beta$ -arrestin 2 distribution in the plasma membrane fractions isolated from HMY-1 and HMY-1/TRPV1 cells that were incubated for 5 min in the absence (Ctrl) and presence of 1  $\mu$ M capsaicin (Caps) or endomorphin-2 (End-2). The figure shows a representative Western blot from four independent experiments. The band intensities were densitometrically evaluated and normalized to  $\beta$ -actin levels. Results represent means  $\pm$  S.E.M. and are expressed as percentage of control (\*\*  $p < 0.01$  versus control). **(B)** Immunofluorescence detection of  $\beta$ -arrestin 2, TRPV1 and MOR in HMY-1 and HMY-1/TRPV1 cells that were incubated for 5 min in the absence (Ctrl) and presence of 1  $\mu$ M capsaicin (Caps) or endomorphin-2 (End-2). After treatment with the agonists, the cells were fixed with 4% PFA and immunostained using primary anti- $\beta$ -arrestin 2 antibody and secondary Alexa Fluor 594-conjugated antibody. Cells were visualized using Zeiss Elyra SP.1 nanoscope equipped with TIRF technology. **(C)** Relative intensity of fluorescence signals corresponding to the amount of  $\beta$ -arrestin 2 associated with the plasma membrane were quantified by Image J software. Results represent means  $\pm$  S.E.M. and are expressed as percentage of control (\*\*  $p < 0.001$  compared to corresponding control).

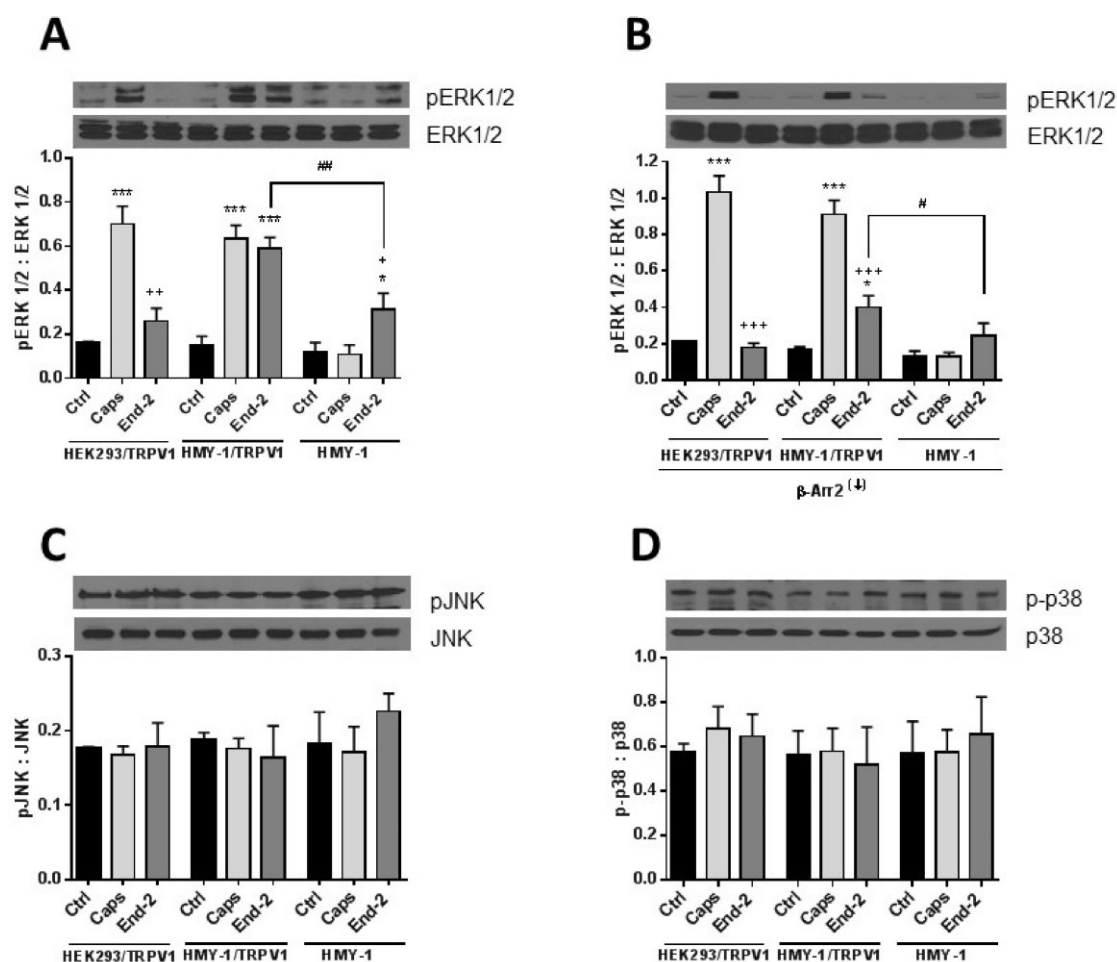


**Figure 8.** Effect of capsaicin and endomorphin-2 on phosphorylation of MAP kinases. HEK293/TRPV1, HMY-1/TRPV1, and HMY-1 cells were incubated for 5 min in the absence (Ctrl) and presence of 1  $\mu$ M capsaicin (Caps) or endomorphin-2 (End-2). In some experiments,  $\beta$ -arrestin 2 was knocked down ( $\beta$ -Arr2( $\downarrow$ )) before treatment of the cells with the agonists. Aliquots of whole cell lysates (30  $\mu$ g protein/lane) were resolved by SDS-PAGE and subjected to immunoblotting using specific antibodies against ERK1/2 and pERK1/2 (A,B), p38 and p-p38 (C), and JNK and pJNK (D). Shown are representative blots from four independent experiments. The band intensities were densitometrically evaluated and normalized to  $\beta$ -actin levels. Results are expressed as means  $\pm$  S.E.M. of the ratios of phosphorylated to unphosphorylated MAPK forms (\*  $p < 0.05$ , \*\*\*  $p < 0.001$  compared to corresponding control; #  $p < 0.05$ , ##  $p < 0.01$  compared to HMY-1/TRPV1; +  $p < 0.05$ , ++  $p < 0.01$ , +++  $p < 0.001$  compared to cells treated with Caps).

### 3. Discussion

The purpose of this study was to investigate the relationship between MOR and TRPV1 and potential crosstalk between their signaling pathways. Using Fluorescent recovery after photobleaching (FRAP), we compared the mobility of both these receptors in the plasma membrane after their activation by capsaicin and endomorphin-2. Capsaicin is a naturally occurring vanilloid that exhibits TRPV1 agonistic activity [15]. Endomorphin-2 is an endogenous MOR agonist biased towards  $\beta$ -arrestin 2-dependent signaling [16,17]. We have previously found that the lateral mobility of MOR in the plasma membrane was significantly increased by DAMGO and decreased by endomorphin-2 [14]. Our current results indicate that the exogenous expression of TRPV1 in HMY-1 cells did not affect the mobility of MOR. However, the activation of TRPV1 with capsaicin markedly increased the mobility of MOR and decreased the number of mobile receptors in the plasma membrane. On the other hand,

we have also observed that the diffusion rate of TRPV1 was changed not only after activation of TRPV1 with capsaicin but also after activation of MOR with endomorphin-2. Interestingly, there were similar changes in mobile fractions of both MOR and TRPV1 after activation with endomorphin-2 or capsaicin. The mobile fractions of both these receptors were decreased after treatment with capsaicin and increased after treatment with endomorphin-2. To date, there is not much information about TRPV1 diffusion in the plasma membrane. It has been reported that the mobility of TRPV1 decreased within seconds upon channel activation in the presence of Ca<sup>2+</sup> [18]. We therefore presume that the decrease in the mobile fraction observed after activation of TRPV1 with capsaicin is due to the certain number of active channels in the plasma membrane.

Our functional studies confirmed that the activation of TRPV1 by capsaicin leads to calcium influx and the activation of MOR by endomorphin-2 suppresses AC activity as reflected by a decrease in cAMP production. Although capsaicin did not affect AC activity and endomorphin-2 did not trigger calcium influx, both these ligands were able to change the mobility of their cognate as well as noncognate receptors in the plasma membrane. These data suggest that these receptors may communicate with each other, but the mechanism is not yet known.

$\beta$ -Arrestins are important proteins that can form scaffolding complexes with a wide variety of proteins in order to regulate diverse signaling pathways [19].  $\beta$ -Arrestin 2 was first identified as a protein capable of mediating desensitization of  $\beta$ 2-adrenergic receptor signaling after agonist stimulation [20]. It is nowadays obvious that  $\beta$ -arrestins play an important role in cell signaling including GPCR desensitization and, rather curiously, may also participate in desensitization of TRPV1 [21]. It was recently shown that the activation of TRPV1 results in nuclear translocation of GRK5, which blocks its ability to phosphorylate MOR, and that this interaction leaves the G protein-mediated analgesic signaling of MOR intact but inhibits  $\beta$ -arrestin 2-mediated internalization and desensitization of MOR [22]. These authors hypothesized that MOR and TRPV1 may compete for GRK5 and  $\beta$ -arrestin 2. Our current observations indicate that  $\beta$ -arrestin 2 is crucially implicated in mediating the relationship between MOR and TRPV1. According to the classical scenario, activation of MOR with endomorphin-2 initiates GRK-catalyzed receptor phosphorylation, which is followed by  $\beta$ -arrestin 2 recruitment to the plasma membrane and binding to the receptor. Consequently, the amount of  $\beta$ -arrestin 2 in the cytoplasm is lowered, which may rather limit its scaffolding function. This could likely explain the observed changes in the diffusion coefficient and mobile fraction of TRPV1.

In order to assess the role of  $\beta$ -arrestin 2 in TRPV1 and MOR cross-communication, we investigated receptors mobility after  $\beta$ -arrestin 2 knockdown. As expected, this intervention increased the mobile fraction of both TRPV1 and MOR in plasma membranes of control (unstimulated) cells. In parallel, the diffusion coefficient of TRPV1 was markedly reduced and there was a downward tendency in the diffusion rate of MOR. The effects of capsaicin and endomorphin-2 on the mobility of both TRPV1 and MOR were notably diminished or altered after  $\beta$ -arrestin 2 knockdown. Interestingly, the study of Por and colleagues [23] demonstrated increased association of unactivated TRPV1 and  $\beta$ -arrestin 2 in CHO cells under normal serum media conditions and reduced association of these two proteins in serum-free media. Here, we observed that treatment of HMY-1/TRPV1 cells with capsaicin for 5 min resulted in a significant decrease in the amount of  $\beta$ -arrestin 2 attached to the plasma membrane. It has been demonstrated that the activation of MOR by some ligands including endomorphin-2 leads to internalization of the MOR- $\beta$ -arrestin 2 complex [17]. Although this event is quite fast, it does not occur within 5 min after MOR activation [24]. It therefore seems plausible that the observed decrease in plasma membrane  $\beta$ -arrestin 2 level is somehow connected with TRPV1 signaling. Our data supports this view: the activation of MOR with endomorphin-2 in HMY-1 cells (not expressing TRPV1) did not reduce the amount of  $\beta$ -arrestin 2 in the plasma membrane. Surprisingly, stimulation of HMY-1/TRPV1 cells with endomorphin-2, similarly as with capsaicin, led to a significant decrement in  $\beta$ -arrestin 2 in the plasma membrane. These observations endorse our hypothesis that there is crosstalk between MOR- and TRPV1-mediated pathways which can play an important role in modulating the receptor signaling.

The MAPK family is a diverse group of proteins involved in ensuring a wide variety of cell physiological processes. They include extracellular signal-regulated kinase (ERK), p38-mitogen activated protein kinase (p38), and c-Jun N-terminal kinase (JNK) [25]. It has been found that the activation of MAPK may participate in generating pain hypersensitivity and that MEK inhibitors known to suppress phosphorylation of ERK can effectively alleviate pain at various time points in several animal models of neuropathic pain [26,27]. It has been reported that stimulation of TRPV1 with capsaicin leads to a rapid phosphorylation and activation of ERK1/2 [28]. Morphine was found to induce ERK activation in CHO cells stably transfected with MOR [29]. It seems evident that MOR can mediate responses in an agonist dependent manner. Agonists such as morphine and methadone activate ERKs via the protein kinase C-dependent pathway but not the  $\beta$ -arrestin-dependent pathway. Contrarily, agonists such as etorphine and fentanyl activate ERKs in a  $\beta$ -arrestin-dependent manner [30]. Previous studies have indicated that morphine and methadone are G protein biased agonists, whereas etorphine, fentanyl, and endomorphin-2 are  $\beta$ -arrestin biased agonists [17]. Interestingly,  $\beta$ -arrestin 2 is not a regulator of phosphorylation of ERK1/2 initiated by activation of some GPCRs [31,32]. Here we show that the cross-communication between the TRPV1 and MOR signaling pathways after activation either by capsaicin or by endomorphin-2 proceeds to ERK1/2. This is clearly evident from our results showing the increase in ERK1/2 phosphorylation after activation of TRPV1 with capsaicin in cells expressing TRPV1. Endomorphin-2 elicited a significant increase in ERK1/2 phosphorylation in cells expressing MOR but, rather surprisingly, a more pronounced increase in ERK1/2 phosphorylation was detected in cells expressing both MOR and TRPV1. Interestingly, Popiolek-Barczyk et al. [33] reported that inhibition of ERK1/2 phosphorylation through inhibiting MEK1/2 (kinase phosphorylating ERK1/2) significantly enhanced the analgesic effects of morphine. It means that phosphorylation of ERK1/2 attenuates analgesia induced by opioids. On the other hand, the p38 MAPK pathway was found to be responsible for more effective analgesia after morphine administration [34]. Here, we observed that TRPV1, which plays a central role in nociception, is of high importance for enhanced phosphorylation of ERK1/2 but not for p38 or JNK phosphorylation in HMY-1/TRPV1 cells following activation of MOR with endomorphin-2. Interestingly,  $\beta$ -arrestin 2 appears to be especially important for MOR-induced ERK1/2 phosphorylation because its downregulation strongly attenuated the ability of endomorphin-2 to increase ERK1/2 phosphorylation. On the other hand, the ability of capsaicin to increase ERK1/2 phosphorylation was not affected by  $\beta$ -arrestin 2 knockdown. These observations suggest that the mechanism of receptor-induced ERK1/2 activation somewhat differ between TRPV1 and MOR.

## 4. Materials and Methods

### 4.1. Cell Culture, Transient Transfection, and Drug Treatment

The human embryonic kidney (HEK) 293 cell line was purchased from Sigma-Aldrich (St. Louis, MI, USA). The HMY-1 cell line (HEK293 cells stably expressing MOR) was prepared and characterized previously [14]. Both cell lines were cultured in Dulbecco's modified Eagle's medium (DMEM) supplemented with 10% fetal bovine serum (FBS) and 1% antibiotic antimycotic solution (AAS, Sigma-Aldrich) at 37 °C in a humidified atmosphere containing 5% CO<sub>2</sub>. For transient transfection, cells were plated in the appropriate multi-well plates and cultivated in the above-mentioned medium. After 24 h, on reaching 60–70% confluence, cells were transfected using Lipofectamine 3000 reagent (Invitrogen, Waltham, MA, USA) according the manufacturer's instructions. Briefly, Lipofectamine 3000 diluted in Opti-MEM medium was mixed with DNA or siRNA diluted in Opti-MEM with P3000 reagent. Final mixture was incubated for 5 min at room temperature and then added directly to the cell culture. After 24 h of incubation, cells were used in further experiments. The plasmid containing TRPV1 with CFP fused to the C-terminus was a generous gift from Dr. Leon D Islas (National Autonomous University of Mexico [35].  $\beta$ -Arrestin 2 siRNA (sc-29208) was purchased from Santa Cruz Biotechnology (Dallas, TX, USA). HMY-1 cells carrying the TRPV1–CFP fusion receptor were denoted HMY-1/TRPV1.

The function of MOR and TRPV1 was modulated by the MOR agonist endomorphin-2 or antagonist naloxone and the TRPV1 agonist capsaicin or antagonist capsazepine. These ligands were dissolved in phosphate-buffered saline (PBS). Before starting the measurement, cells were incubated for 5 min either with endomorphin-2 (1  $\mu\text{M}$ ) or capsaicin (0.5  $\mu\text{M}$ ) or naloxone (10  $\mu\text{M}$ ) or capsazepine (5  $\mu\text{M}$ ). In some cases, cells were pretreated for 10 min with naloxone (10  $\mu\text{M}$ ) or capsazepine (5  $\mu\text{M}$ ) and then exposed for 5 min to endomorphin-2 (1  $\mu\text{M}$ ) or capsaicin (0.5  $\mu\text{M}$ ), respectively.

#### 4.2. Total Internal Reflection (TIRF)

Cells were plated on a 35 mm glass-bottom dishes in phenol red-free DMEM supplemented with 10% FBS and 1% AAS. After 24 h, cells were transfected with plasmid cDNA encoding the CFP-tagged TRPV1 receptor as described above. One day after transfection, cells were visualized using Zeiss Elyra SP.1 nanoscope equipped with TIRF technology.

#### 4.3. Fluorescent Recovery after Photobleaching

HMY-1/TRPV1 cells were seeded on glass-bottom dishes and maintained in phenol red-free DMEM supplemented with 10% FCS, 1% AAS, and 0.8 mg/mL geneticin. FRAP experiments on living cells were performed on an inverted Zeiss LSM 880 confocal laser scanning microscope (Carl Zeiss AG, Oberkochen, Germany) equipped with 40 $\times$ /1.2 WDICIII C Apochromat objective lens and back-thinned CCD camera (Zeiss Axio Cam). For excitation of fluorophores, we used the 514-nm laser for visualizing YFP and 405-nm laser for visualizing CFP. Images were acquired using ZEN Black software (Carl Zeiss AG). During all FRAP experiments, the cells were placed in a chamber providing a stable temperature 37  $^{\circ}\text{C}$  and 5%  $\text{CO}_2$ . All the diffusion data was always assessed by FRAP measurements in plasma membrane areas adjacent to the glass support. Bleaching (six iterations per bleach) was accomplished with a circular spot with 2- $\mu\text{m}$  radius using the 488- and 514-nm for YFP and 458- and 488-nm for CFP laser pulse from a 40-mW Argon laser operating at 100% power. The time course of the fluorescence recovery signal after photobleaching was monitored at low laser intensity (2% of maximum power) and 512  $\times$  512 pixels resolution with sampling rate of 2 ms. In each FRAP series, 15 prebleach images were collected and, immediately after photobleaching, 400 successive postbleach images were recorded to monitor the fluorescence redistribution. FRAP curves were normalized to the prebleach value of the respective pulse train. The data obtained from at least 50 cells (screened in three individual runs) during each FRAP experiment were analyzed using easyFRAP, a MATLAB platform-based tool [36]. Recovery curves were calculated according to the following equation:

$$\text{recovery (\%)} = (I_{\text{bleach}} - I_{\text{bckg}}) / (I_{\text{ref}} - I_{\text{bckg}}) \times 100$$

where  $I_{\text{bleach}}$  is the fluorescence intensity of the bleached spot,  $I_{\text{bckg}}$  is the fluorescence intensity of the background, and  $I_{\text{ref}}$  is the fluorescence intensity of the control regions in other cells or regions far remote from the target cell. The values of the apparent diffusion coefficients ( $D$ ) for both receptors were obtained from the following equation:

$$D = 0.224 \omega^2 / t_{1/2}$$

where  $\omega$  is the diameter of the selected bleached spot and  $t_{1/2}$  is the half-life of the fluorescence recovery [37].

The potential effects of agonists on the lateral mobility of MOR–YFP or TRPV1–CFP were investigated using endomorphin-2 and capsaicin. HMY1/TRPV1 cells were pretreated for 5 min with individual agonists and the agonists were left in the medium during the whole experiment. Antagonists of MOR and TRPV1 receptors (naloxone and capsazepine, respectively) were applied to cells 10 min before adding agonists and they were used at final concentrations 10 times higher than those of agonists.

#### 4.4. Time Resolved Fluorescence Assay for cAMP

The direct quantitative determination of cAMP in cells affected by receptor ligands was performed using cAMP-Gi kit (Cisbio Bioassays, Parc Marcel Boiteux, Codolet, France) based on HTRF<sup>®</sup> technology (Homogenous Time Resolved Fluorescence). Cells were seeded in a 384-well plate (8000 cells per well), transfected in 24 h, and the assay was performed after 24 h of incubating the cells with complex of Lipofectamine 3000-TRPV1 DNA plasmid. Cells were incubated for 20 min at 37 °C and 5% CO<sub>2</sub> in the presence of ligands diluted to a final concentration 1 μM in stimulation buffer. Forskolin at a concentration 2 μM was added before incubating the cells for 45 min at 37 °C. Then cryptate-labeled cAMP and monoclonal anti-cAMP-d2 antibody diluted in lysis and detection buffer were added. The plate was incubated for 1 h at room temperature before transferring the final lysate to a white 96-well plate and reading absorbance at 620 and 665 nm in Tecan Safire 2 reader.

#### 4.5. Endpoint Calcium Assay

Cells were seeded in a 384-well plate (8000 cells per well) and after 24 h transfected with the TRPV1-CFP plasmid. After the next 24 h, cells were used for the assay. We used Cell Meter<sup>TM</sup> No Wash and Probenecid-Free Endpoint Calcium Assay kit (AAT Bioquest). Fluo-8ETM AM dye solution was prepared according to the manufacturer's instructions and mixed with assay buffer. Then, 25 μL per well of the mixture was added to the plate and incubated for 45 min at 37 °C. After the incubation, agonist resuspended in HHBS buffer was added and the calcium flux assay was run immediately. The fluorescence intensity at Ex/Em = 490/525 nm was monitored on a microplate reader (bottom read mode).

#### 4.6. Isolation of a Plasma Membrane Fraction

Transfected and non-transfected (control) cells were incubated in the presence or absence of ligands at 37 °C for 5 min. The cells were immediately chilled in an ice bath and harvested in TMES buffer (20 mM Tris, 3 mM MgCl<sub>2</sub>, 1 mM EDTA, 250 mM sucrose; pH 7.4). The plasma membrane fraction was isolated using Percoll<sup>®</sup> self-forming gradient as previously described with some modifications [38]. Cell homogenates (3 mL) were loaded on the top of 23 mL of 18% Percoll solution in TMES buffer and centrifuged in a Beckman Ti50 rotor at 60,000× g for 15 min. The resulting upper layer enriched in plasma membranes was collected, diluted in TME buffer (20 mM Tris, 3 mM MgCl<sub>2</sub>, 1 mM EDTA; pH 7.4), and centrifuged at 150,000× g for 1 h. The pellet was resuspended in TME buffer, frozen in liquid nitrogen, and stored at −80 °C.

#### 4.7. SDS-PAGE and Immunoblotting

Samples were solubilized in Laemmli buffer and loaded on standard 10% acrylamide gels for SDS-PAGE. The resolved proteins were transferred to nitrocellulose membrane, blocked with 5% non-fat dry milk in TBS buffer (10 mM Tris, 150 mM NaCl; pH 8.0) for 30 min, and then incubated in the presence of relevant primary antibodies with gentle agitation overnight at 4 °C. After three 10-min washes in TBS containing 0.3% Tween 20 (TBS-Tween), the secondary antibodies labeled with horseradish peroxidase were applied for 1 h at room temperature. After another three 10-min washes in TBS-Tween, the blots were visualized by enhanced chemiluminescence technique according to the manufacturer's instructions (Pierce Biotechnology, Rockford, IL, USA). The immunoblots were scanned and quantitatively analyzed by ImageJ software.

#### 4.8. Immunofluorescence

Cells were plated in 35 mm glass bottom dishes and were cultured in phenol red-free DMEM supplemented with 10% FBS and 1% AAS for 24 h prior to transfection with TRPV1-CFP construct as described above. The following day, cells were fixed with 4% paraformaldehyde for 15 min at room temperature. Cells were washed three times in PBS and permeabilized with 0.2% Triton in PBS

for 5 min. Samples were blocked with 10% donkey serum and 1% BSA in PBS for 1 h and then washed three times and incubated with primary antibody against  $\beta$ -arrestin 2 for 1 h. Cells were washed three times with PBS and incubated for 1 h with secondary donkey anti-rabbit antibody (Alexa Fluor 594, Life Technologies). After incubation, cells were washed three times with PBS and visualized using Zeiss Elyra SP.1 nanoscope enabling live-cell imaging and TIRF illumination.

#### 4.9. Materials

Lipofectamine 3000 was purchased from Invitrogen (Carlsbad, CA, USA) and fetal bovine serum (FBS) was from Thermo Fisher Scientific (Waltham, MA, USA). HTRF cAMP Gi Assay kit was purchased from Cisbio Bioassays (Barford, MA, USA) and Cell Meter™ No Wash and Probenecid-Free Endpoint Calcium Assay kit was from AAT Bioquest (Sunnyvale, CA, USA).  $\beta$ -Arrestin 2 antibody was from ThermoFisher Scientific, ERK1/2, p-ERK1/2, JNK, and pJNK antibodies were from Cell Signaling Technology (Beverly, MA) and p38 and p-p38 antibodies were from Santa Cruz Biotechnology. All the ligands and other chemicals were purchased from Sigma-Aldrich (St. Louis, MI, USA) and they were of the highest purity available.

#### 4.10. Statistics

Data are expressed as mean values  $\pm$  standard error of the mean (S.E.M.) of at least three independent experiments. All statistical analyses were conducted using GraphPad Prism, Version 6.0 (GraphPad Software Inc., La Jolla, CA, USA). The differences between the means of relevant groups were statistically evaluated by one-way ANOVA followed by the Bonferroni post hoc test. Significance level was set at  $p \leq 0.05$ .

## 5. Conclusions

Taken together, our results indicate that not only the activation of one receptor influences the other one but that the mere presence of one receptor can modulate the signaling properties of the other receptor. To date, there is no information about the possible formation of dimers between TRPV1 and MOR in the plasma membrane. The different lateral mobility properties of both these receptors insinuate that this option is rather unlikely. Nevertheless, the present data clearly demonstrate that capsaicin and endomorphin-2 may both influence the behavior of TRPV1 and MOR in the plasma membrane and shed some new light on the possible cross-communication between these two receptors and their signaling pathways.

**Author Contributions:** B.M., V.M., and L.H. performed all the experiments and data analysis. J.N. supervised the project, provided funding for the study, and wrote the manuscript. All authors have read and agreed to the published version of the manuscript.

**Funding:** This work was supported by the Charles University, project GA UK No. 790217 and 1196120, institutional project SVV-260434/2020 and cofinanced by the European Regional Development Fund and the state budget of the Czech Republic (CZ.1.05/4.1.00/16.0347 and CZ.2.16/3.1.00/21515).

**Conflicts of Interest:** The authors declare no conflict of interest. The funders had no role in the design of the study; in the collection, analyses, or interpretation of data; in the writing of the manuscript, or in the decision to publish the results.

## References

1. Spetea, M.; Asim, M.F.; Wolber, G.; Schmidhammer, H. The  $\mu$  opioid receptor and ligands acting at the  $\mu$  opioid receptor, as therapeutics and potential therapeutics. *Curr. Pharm. Des.* **2013**, *19*, 7415–7434. [[CrossRef](#)] [[PubMed](#)]
2. Pergolizzi, J.V.; LeQuang, J.A.; Taylor, R.; Ossipov, M.H.; Colucci, D.; Raffa, R.B. Designing safer analgesics: A focus on  $\mu$ -opioid receptor pathways. *Expert Opin. Drug Discov.* **2018**, *13*, 965–972. [[CrossRef](#)]
3. Lopez-Gimenez, J.F.; Milligan, G. Opioid regulation of mu receptor internalisation: Relevance to the development of tolerance and dependence. *CNS Neurol. Disord. Drug Targets* **2010**, *9*, 616–626. [[CrossRef](#)]

4. Mizoguchi, H.; Watanabe, C.; Sakurada, T.; Sakurada, S. New vistas in opioid control of pain. *Curr. Opin. Pharmacol.* **2012**, *12*, 87–91. [[CrossRef](#)]
5. Burford, N.T.; Traynor, J.R.; Alt, A. Positive allosteric modulators of the  $\mu$ -opioid receptor: A novel approach for future pain medications. *Br. J. Pharmacol.* **2015**, *172*, 277–286. [[CrossRef](#)]
6. Vetter, I.; Wyse, B.D.; Monteith, G.R.; Roberts-Thomson, S.J.; Cabot, P.J. The mu opioid agonist morphine modulates potentiation of capsaicin-evoked TRPV1 responses through a cyclic AMP-dependent protein kinase A pathway. *Mol. Pain* **2006**, *2*, 22. [[CrossRef](#)] [[PubMed](#)]
7. Endres-Becker, J.; Heppenstall, P.A.; Mousa, S.A.; Labuz, D.; Oksche, A.; Schäfer, M.; Stein, C.; Zöllner, C. Mu-opioid receptor activation modulates transient receptor potential vanilloid 1 (TRPV1) currents in sensory neurons in a model of inflammatory pain. *Mol. Pharmacol.* **2007**, *71*, 12–18. [[CrossRef](#)] [[PubMed](#)]
8. Premkumar, L.S.; Abooj, M. TRP channels and analgesia. *Life Sci.* **2013**, *92*, 415–424. [[CrossRef](#)] [[PubMed](#)]
9. Roberts, J.C.; Davis, J.B.; Benham, C.D. [3H] Resiniferatoxin autoradiography in the CNS of wild-type and TRPV1 null mice defines TRPV1 (VR-1) protein distribution. *Brain Res.* **2004**, *995*, 176–183. [[CrossRef](#)]
10. Messeguer, A.; Planells-Cases, R.; Ferrer-Montiel, A. Physiology and pharmacology of the vanilloid receptor. *Curr. Neuropharmacol.* **2006**, *4*, 1–15. [[CrossRef](#)]
11. Studer, M.; McNaughton, P.A. Modulation of single-channel properties of TRPV1 by phosphorylation. *J. Physiol.* **2010**, *588*, 3743–3756. [[CrossRef](#)] [[PubMed](#)]
12. Maione, S.; Starowicz, K.; Cristino, L.; Guida, F.; Palazzo, E.; Luongo, L.; Rossi, F.; Marabese, I.; de Novellis, V.; Di Marzo, V. Functional interaction between TRPV1 and mu-opioid receptors in the descending antinociceptive pathway activates glutamate transmission and induces analgesia. *J. Neurophysiol.* **2009**, *101*, 2411–2422. [[CrossRef](#)] [[PubMed](#)]
13. Bao, Y.; Gao, Y.; Yang, L.; Kong, X.; Yu, J.; Hou, W.; Hua, B. The mechanism of  $\mu$ -opioid receptor (MOR)-TRPV1 crosstalk in TRPV1 activation involves morphine anti-nociception, tolerance and dependence. *Channels* **2015**, *9*, 235–243. [[CrossRef](#)] [[PubMed](#)]
14. Melkes, B.; Hejnova, L.; Novotny, J. Biased  $\mu$ -opioid receptor agonists diversely regulate lateral mobility and functional coupling of the receptor to its cognate G proteins. *Naunyn Schmiedebergs Arch. Pharmacol.* **2016**, *389*, 1289–1300. [[CrossRef](#)]
15. Ho, K.W.; Ward, N.J.; Calkins, D.J. TRPV1: A stress response protein in the central nervous system. *Am. J. Neurodegener. Dis.* **2012**, *1*, 1–14.
16. McPherson, J.; Rivero, G.; Baptist, M.; Llorente, J.; Al-Sabah, S.; Krasel, C.; Dewey, W.L.; Bailey, C.P.; Rosethorne, E.M.; Charlton, S.J.; et al. mu-Opioid Receptors: Correlation of Agonist Efficacy for Signalling with Ability to Activate Internalization. *Mol. Pharmacol.* **2010**, *78*, 756–766. [[CrossRef](#)]
17. Rivero, G.; Llorente, J.; McPherson, J.; Cooke, A.; Mundell, S.J.; McArdle, C.A.; Rosethorne, E.M.; Charlton, S.J.; Krasel, C.; Bailey, C.P.; et al. Endomorphin-2: A Biased Agonist at the mu-Opioid Receptor. *Mol. Pharmacol.* **2012**, *82*, 178–188. [[CrossRef](#)]
18. Senning, E.N.; Gordon, S.E. Activity and  $\text{Ca}^{2+}$  regulate the mobility of TRPV1 channels in the plasma membrane of sensory neurons. *Elife* **2015**, *4*, e03819. [[CrossRef](#)]
19. Smith, J.S.; Rajagopal, S. The  $\beta$ -Arrestins: Multifunctional Regulators of G Protein-coupled Receptors. *J. Biol. Chem.* **2016**, *291*, 8969–8977. [[CrossRef](#)]
20. Lohse, M.J.; Benovic, J.L.; Codina, J.; Caron, M.G.; Lefkowitz, R.J. beta-Arrestin: A protein that regulates beta-adrenergic receptor function. *Science* **1990**, *248*, 1547–1550. [[CrossRef](#)]
21. Por, E.D.; Bierbower, S.M.; Berg, K.A.; Gomez, R.; Akopian, A.N.; Wetsel, W.C.; Jeske, N.A.  $\beta$ -Arrestin-2 desensitizes the transient receptor potential vanilloid 1 (TRPV1) channel. *J. Biol. Chem.* **2012**, *287*, 37552–37563. [[CrossRef](#)] [[PubMed](#)]
22. Scherer, P.C.; Zaccor, N.W.; Neumann, N.M.; Vasavda, C.; Barrow, R.; Ewald, A.J.; Rao, F.; Sumner, C.J.; Snyder, S.H. TRPV1 is a physiological regulator of  $\mu$ -opioid receptors. *Proc. Natl. Acad. Sci. USA* **2017**, *114*, 13561–13566. [[CrossRef](#)] [[PubMed](#)]
23. Por, E.D.; Gomez, R.; Akopian, A.N.; Jeske, N.A. Phosphorylation regulates TRPV1 association with  $\beta$ -arrestin-2. *Biochem. J.* **2013**, *451*, 101–109. [[CrossRef](#)] [[PubMed](#)]
24. Williams, J.T.; Ingram, S.L.; Henderson, G.; Chavkin, C.; von Zastrow, M.; Schulz, S.; Koch, T.; Evans, C.J.; Christie, M.J. Regulation of  $\mu$ -opioid receptors: Desensitization, phosphorylation, internalization, and tolerance. *Pharmacol. Rev.* **2013**, *65*, 223–254. [[CrossRef](#)] [[PubMed](#)]

25. Widmann, C.; Gibson, S.; Jarpe, M.B.; Johnson, G.L. Mitogen-activated protein kinase: Conservation of a three-kinase module from yeast to human. *Physiol. Rev.* **1999**, *79*, 143–180. [[CrossRef](#)]
26. Obata, K.; Noguchi, K. MAPK activation in nociceptive neurons and pain hypersensitivity. *Life Sci.* **2004**, *74*, 2643–2653. [[CrossRef](#)] [[PubMed](#)]
27. Ma, W.; Quirion, R. The ERK/MAPK pathway, as a target for the treatment of neuropathic pain. *Expert Opin. Ther. Targets* **2005**, *9*, 699–713. [[CrossRef](#)]
28. Backes, T.M.; Rössler, O.G.; Hui, X.; Grötzinger, C.; Lipp, P.; Thiel, G. Stimulation of TRPV1 channels activates the AP-1 transcription factor. *Biochem. Pharmacol.* **2018**, *150*, 160–169. [[CrossRef](#)]
29. Li, L.Y.; Chang, K.J. The stimulatory effect of opioids on mitogen-activated protein kinase in Chinese hamster ovary cells transfected to express mu-opioid receptors. *Mol. Pharmacol.* **1996**, *50*, 599–602.
30. Zheng, H.; Loh, H.H.; Law, P.Y. beta-arrestin-dependent mu-opioid receptor-activated extracellular signal-regulated kinases (ERKs) translocate to nucleus in contrast to G protein-dependent ERK activation. *Mol. Pharmacol.* **2008**, *73*, 178–190. [[CrossRef](#)]
31. Jin, M.; Min, C.; Zheng, M.; Cho, D.I.; Cheong, S.J.; Kurose, H.; Kim, K.M. Multiple signaling routes involved in the regulation of adenylyl cyclase and extracellular regulated kinase by dopamine D-2 and D-3 receptors. *Pharmacol. Res.* **2013**, *67*, 31–41. [[CrossRef](#)] [[PubMed](#)]
32. Jain, R.; Watson, U.; Saini, D.K. ERK activated by Histamine H1 receptor is anti-proliferative through spatial restriction in the cytosol. *Eur. J. Cell Biol.* **2016**, *95*, 623–634. [[CrossRef](#)] [[PubMed](#)]
33. Popiolek-Barczyk, K.; Makuch, W.; Rojewska, E.; Pilat, D.; Mika, J. Inhibition of intracellular signaling pathways NF-kappa B and MEK1/2 attenuates neuropathic pain development and enhances morphine analgesia. *Pharmacol. Rep.* **2014**, *66*, 845–851. [[CrossRef](#)] [[PubMed](#)]
34. Yamdeu, R.S.; Shaqura, M.; Mousa, S.A.; Schafer, M.; Droese, J. p38 Mitogen-activated Protein Kinase Activation by Nerve Growth Factor in Primary Sensory Neurons Upregulates mu-Opioid Receptors to Enhance Opioid Responsiveness Toward Better Pain Control. *Anesthesiology* **2011**, *114*, 150–161. [[CrossRef](#)] [[PubMed](#)]
35. De-la-Rosa, V.; Rangel-Yescas, G.E.; Ladrón-de-Guevara, E.; Rosenbaum, T.; Islas, L.D. Coarse architecture of the transient receptor potential vanilloid 1 (TRPV1) ion channel determined by fluorescence resonance energy transfer. *J. Biol. Chem.* **2013**, *288*, 29506–29517. [[CrossRef](#)] [[PubMed](#)]
36. Rapsomaniki, M.A.; Kotsantis, P.; Symeonidou, I.-E.; Giakoumakis, N.-N.; Taraviras, S.; Lygerou, Z. easyFRAP: An interactive, easy-to-use tool for qualitative and quantitative analysis of FRAP data. *Bioinformatics* **2012**, *28*, 1800–1801. [[CrossRef](#)] [[PubMed](#)]
37. Soumpasis, D.M. Theoretical analysis of fluorescence photobleaching recovery experiments. *Biophys. J.* **1983**, *41*, 95–97. [[CrossRef](#)]
38. Hejnova, L.; Skrabalova, J.; Novotny, J. Prolonged Morphine Treatment Alters Expression and Plasma Membrane Distribution of  $\beta$ -Adrenergic Receptors and Some Other Components of Their Signaling System in Rat Cerebral Cortex. *J. Mol. Neurosci.* **2017**, *63*, 364–376. [[CrossRef](#)]

